CHALMERS
UNIVERSITY OF TECHNOLOGY

Signal Analysis of Gamma Brain Oscillations Recorded with Low-T_c and High-T_c SQUID-Based Magnetoencephalography

A Matching Pursuit Approach

Master's Thesis

Author

TAMARA GOUDIAN

Supervisors

ELENA OREKHOVA
JUSTIN SCHNEIDERMAN

Department of Electrical Engineering
Master Program in Biomedical Engineering
Chalmers University of Technology
Gothenburg, Sweden May 29, 2019

MASTER'S THESIS 2019 | REPORT NO.:

Signal Analysis of Gamma Brain Oscillations Recorded with Low-T_c and High-T_c SQUID-Based Magnetoencephalography

A Matching Pursuit Approach

TAMARA GOUDIAN

Department of Electrical Engineering
Master Program in Biomedical Engineering
CHALMERS UNIVERSITY OF TECHNOLOGY
Gothenburg, Sweden 2019

Signal Analysis of Gamma Brain Oscillations Recorded with Low-T_c and High-T_c SQUID-Based Magnetoencephalography
A Matching Pursuit Approach
TAMARA GOUDIAN

This publication has been produced during my scholarship period at Chalmers University of Technology, funded by the Swedish Institute. The project was also carried out in collaboration with MedTech West.

Supervisors:

Dr. Elena Orekhova
Institute of Neuroscience and Physiology, Sahlgrenska Academy

Dr. Justin Schneiderman
Dept. of Microtechnology and Nanoscience, Chalmers University of Technology

Examiner:
Justin Schneiderman
Dept. of Microtechnology and Nanoscience, Chalmers University of Technology

Master's Thesis 2019 | Report No.:
Department of Electrical Engineering
Master Program in Biomedical Engineering
Chalmers University of Technology
SE-412 96 Gothenburg, Sweden
Telephone +46 (0)31-772 10 00

Typeset in LaTeX
Printed by Chalmers Reproservice
Gothenburg, Sweden 2019

Signal Analysis of Gamma Brain Oscillations Recorded with Low-T_c and High-T_c SQUID-Based Magnetoencephalography
A Matching Pursuit Approach
TAMARA GOUDIAN
Dept. of Electrical Engineering, Master Program in Biomedical Engineering
Chalmers University of Technology

Abstract

Brain diseases present a growing social and economic burden worldwide. However, understanding the pathogenesis leading to many such diseases remains a great challenge. Magnetoencephalography (MEG) is a promising safe and non-invasive imaging technique with demonstrated utility in several research and clinical neuroscience applications. Most of the common MEG devices detect magnetic signals emitted from the brain using highly sensitive sensors - superconducting quantum interference devices (SQUIDs) - that operate below a specific temperature known as the critical temperature (T_c). To support the usefulness of MEG, suitable analysis techniques are needed to extract meaningful information from MEG recordings. Several standard time-frequency analysis techniques have been used for this purpose but impose a trade-off between frequency and time resolutions making it difficult to capture transient and rhythmic components of signals simultaneously. One technique that offers improvement with this respect is Matching Pursuit (MP).

This project explores the MP algorithm as an option for the analysis of brain oscillations in MEG recordings obtained from human subjects following. This is motivated by its success when applied to electroencephalography (EEG) recordings from monkeys in recent research efforts. Here, MP is used to study gamma oscillations, which are associated with cortical functions involving high-level cognitive and sensory processes. Two implementations were investigated: one using a dyadic dictionary, and the second using a stochastic dictionary. The aim is to test MP's capacity to extract different or new information from MEG recordings: first differences in data obtained from low-T_c SQUID-based devices and high-T_c SQUID-based devices, and then differences between human subjects with and without autism spectrum disorders (ASD). The results of both tests reveal some insightful differences that may form a basis for further investigation. Nonetheless, further efforts are needed to examine other implementations of MP to provide better accuracy and performance for use in clinical settings. Overall, there is a need to provide enhanced analysis methods and more solid interpretations of their outputs.

Keywords: Magnetoencephalography, Time-Frequency Analysis, Matching Pursuit, Dyadic Dictionary, Stochastic Dictionary, Low-T_c SQUIDs, High-T_c SQUIDs, On-Scalp MEG, Autism Spectrum Disorders.

Acknowledgements

First, I would like to thank my thesis supervisors. Dr. Justin Schneiderman affiliated scientist at the Quantum Device Physics Laboratory (department of Microtechnology and Nanoscience, Chalmers University of Technology), for granting me the opportunity to work on this project and for his guidance and support. Dr. Elena Orekhova, researcher at the Gillberg Neuropsychiatry Centre (Institute of Neuroscience and Physiology, Sahlgrenska Academy), for her continuous guidance and mentorship.

I am grateful to Christoph Pfeiffer (PhD student, Quantum Device Physics Laboratory, Microtechnology and Nanoscience, Chalmers University of Technology) for providing guidance and relevant tutorials. I am also very thankful for the technical assistance I received from Dr. Bushra Riaz (researcher at MedTech West). I would also like to acknowledge my fellow Master students and opponents Linh Nguyen and Mattias Karlsson for the thesis review and valuable feedback.

Furthermore, a lot of gratitude goes out to to Dr. Supratim Ray and Dr. Subhash Chandran KS for making their source code public and for the information they provided during this project.

Next, I would like to thank Henrik Mindedal (Director at MedTech West) for connecting me with MedTech West and Dr. Dag Winkler (Professor at the Department of Microtechnology and Nanoscience, University of Chalmers) for taking the time to familiarize me with the Quantum Device Physics Laboratory. I am also very grateful to MedTech West for hosting this project and providing all necessary resources. I have received a lot of support from everyone there.

Moreover, I would like to express my gratitude to the director of the Biomedical Engineering programme, Ants Silberberg (department of Electrical Engineering, Chalmers University of Technology) and all professors, lecturers, teaching assistants, and administrative staff for all their efforts over the past two years.

I would also like to acknowledge my school (Sisters of Nazareth School) and the University of Jordan for the quality education provided. I would especially like to mention Dr. Andraws Swidan and Dr. Souheil Odeh for their belief in my abilities, their guidance, and support.

I cannot express enough my very profound love and gratitude to my mother, father, and little sister for their unfailing love, my uncles Sami and Tawfic Ghandour for their support and encouragement, and my friends for their friendship and continuous encouragement.

Last but not least I would like to thank the Swedish Institute not only for the opportunity to study in Sweden and engage with the Network of Future Global Leaders (NFGL) but also for the sincere support from everyone working there.

Abbreviations and Acronyms

- ASD: Autism Spectrum Disorders
- DFT: Discrete Fourier Transform
- EEG: Electroencephalography
- E-I: excitation-inhibition.
- FT: Fourier Transform
- T_c: Critical Temperature
- Hz: Hertz
- MEG: Magnetoencephalography
- mm: Millimeter
- MP: Matching Pursuit
- MRI: Magnetic Resonance Imaging
- MT: Multitaper
- NT: Neurotypical
- PAC: Phase Amplitude Coupling
- PET: Positron Emission Tomography
- PSD: power spectral density
- s: Second
- SPECT: Single Photon Emission Computed Tomography
- SQUID: Superconducting Quantum Interference Devices
- STFT: Short-Time Fourier Transform
- T: Tesla
- TF: Time-Frequency
- WT: Wavelet Transform
- WVD: Wigner-Ville Distribution
- 2D: Two-Dimensional

Contents

1 Introduction

Brain diseases constitute a substantial social and economic burden worldwide [1][2]. In Europe alone, the number of afflicted people was estimated to be around 179 million in 2010 [2]. In 2015, the Global Burden of Disease study revealed that around one third of the world's population is affected by neurological or mental disorders throughout their lifetime. European studies indicate that disorders of the brain account for 35% of Europe's total disease burden with an annual cost of 800 billion euros. These numbers are continuously rising due to the increase in life expectancy, the prevalence of chronic diseases, in addition to other socioeconomic factors [1].

While neuroscience is at the forefront of research efforts, a great deal remains to be understood with regards to brain functions at all levels - molecular, cellular, and systematic - to uncover the complex pathogenesis of brain diseases. This in turn requires new and enhanced techniques and technologies to study the brain. Recent development is beginning to demonstrate the usefulness of magnetoencephalography (MEG) in both basic and clinical neuroscience especially as a generally safe non-invasive imaging technique [3].

As with any imaging tool, one challenge that the MEG technology faces is the development of suitable analysis methods to extract meaningful information that may be used for the diagnosis and treatment of brain-related disease. MEG data is analyzed using several techniques, one of which is time-frequency analysis [4] which may come in several different flavours and implementations. In this project, a time-frequency analysis method known as Matching Pursuit (MP) is investigated along with the possible improvements it brings when compared to other standard methods used for MEG signal analysis [5]. Also, possible applications of this technique are explored to evaluate its usefulness and capacity to uncover distinct characteristics in different MEG datasets. One application involves the comparison of conventional MEG systems and a new on-scalp MEG system that is currently being developed [6]. The other studies the possibility of finding distinctive features that differentiate human subjects with autism spectrum disorders from those without.

This report summarizes the project and its results. First, background material is presented starting with an overview about the brain and neural activity, followed by an introduction to MEG and relevant analysis techniques with a focus on the MP method, and ending with a description of the aims and objectives of the project. Then the methods used to produce the results are outlined. Afterwards, the results are presented and described. The report concludes with a discussion and a conclusion based on the current findings. Supplementary information is attached in the appendix and the software used and output of experiments are made accessible via links provided in the methods and results sections.

1.1 The Brain and Neural Oscillations

The main focus of this project is the analysis of the magnetic waves generated by the brain that are detectable outside the head by magnetoencephalography devices, which are described in the following section.

The brain [7] is one of the most vital organs of the human body and the central organ of the nervous system. It is responsible for controlling most functions in the body by receiving and processing information, making decisions, and issuing instructions to the rest of the body among other activities. It consists of around 100 billion neurons (nerve cells) and 10-50 trillion neuroglia (supporting cells).

Neurons [7] are electrically excitable cells that are specialized in processing and communicating cellular signals. At any instant, millions of nerve impulses are fired by these neurons. Neural oscillations [8][9] are rhythmic patterns of neural activity that are driven by processes within individual neurons or interactions between different neurons. Synchronizations may also occur in populations of nerve cells involved in a certain neural computation and their rhythmic changes add up giving rise to large-scale oscillations that are detectable outside the scalp.

Externally detectable waves are generated by neurons lying close to the brain surface mainly in the cerebral cortex, which is the outer layer of the largest part of the brain known as the cerebrum. There, a special group of neural cells, known as pyramidal cells, play an essential role in the generation of the magnetic signals emitted by the brain [3]. Neural activity results in electrical currents that are caused by action potentials occurring due to a rapid increase or decrease in membrane potentials. The membrane potential is the difference in electric potential between the interior and the exterior of a cell driven by the flow of ions across the cell membrane [7]. Therefore, when pyramidal neurons are activated, this causes intracellular and extracellular currents to flow. When considering the dendrite of such pyramidal neurons as a long cylinder, the longitudinal components of these currents add up, while the transverse components cancel out. This results in a current along the main axes of the neurons and magnetic induction that circulates around the current flow as shown in figure 1. The sources of this magnetic induction are the postsynaptic potentials (PSPs) occurring at synapses (neuronal junctions) with fast spikes and slower components, and axonal discharges or action potentials (APs) propagating along the neuron's axon. It is mainly the mass effect of the slow components of PSPs in the pyramidal cells that generates the currents that induce the magnetic induction. The elongated shape of the pyramidal cells and the parallel arrangement of the main axes of their dendritic trees enhance its strength. A minimum of 10000-50000 adjacent parallel neurons activated simultaneously are needed to generate a magnetic signal outside the brain that may be picked up and recorded by MEG devices [3][10].

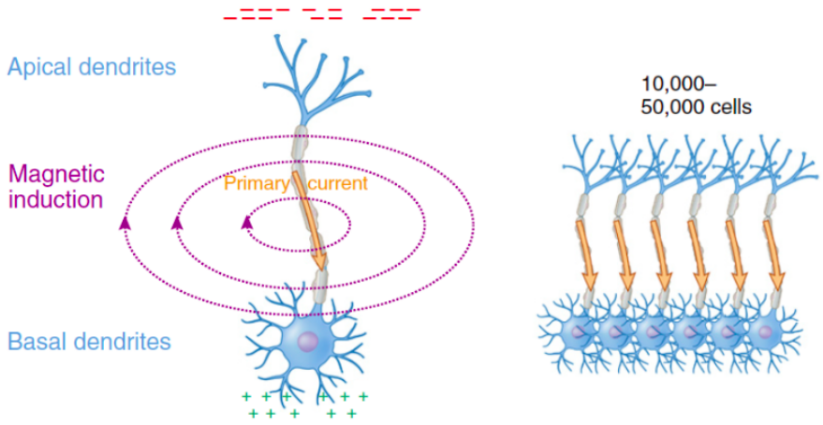

Figure 1: Pyramidal cells and neural activity. Left: neural activity results in a net current along the axon and magnetic induction circulating around the current. Right: Assembly of parallel pyramidal cells activated concurrently. Image adapted from Baillet, 2017 [3].

Neural oscillations have been associated with various sensory and cognitive functions and therefore can provide valuable insights to healthcare professionals [8]. Signals from the brain show rhythmic patterns at different frequencies and have been grouped into different bands: delta 1–4 Hz, theta 4–8 Hz, alpha 8–12 Hz, beta 13–30 Hz, low gamma 30–70 Hz, and high gamma 70–150 Hz [9]. These rhythms are connected to internal processes of the brain in addition to external stimuli. They also contain highly transient components arising from spikes or sudden onsets of stimuli with durations that are less than tens of milliseconds (ms). Both internal states and external stimuli may change over short intervals of time causing brain signals to be highly non-stationary. Therefore, methods used for the analysis of MEG recordings need be able to capture both transient and rhythmic components of the signals [5].

This project is mainly concerned with gamma rhythms with a center frequency of 30–80 hertz (Hz). These rhythms have been associated with cortical functions involving high-level cognitive and sensory processes [5]. They have also been found to play an essential role in the brain's response to visual stimuli [8]. Gamma waves show two types of responses: an early transient response and a later 'induced gamma' response to visual stimulation. Each type conveys different information; the early gamma component fulfills sensory functions and the late gamma component fulfills perceptual-cognitive functions [11]. Furthermore, these oscillations arise from the interaction between neural excitation (E) and inhibition (I). E–I balance in neural networks is essential for normal cortical function. In neurological disorders such as epilepsy or autism, this balance can be disrupted. Therefore, gamma waves may provide a non-invasive window to understand and monitor the state of E-I balance in human cortical networks and may be promising markers for the diagnosis and treatment of such diseases. This could also provide a measure for patients with elevated cortical excitability and high sensitivity to certain stimuli and aid in tracking the effects of pharmacological interventions in clinical trials targeting this patient category [12].

1.2 Magnetoencephalography (MEG)

Magnetoencephalography [6] is a functional neuroimaging technique used to capture and study neural activity as reflected by the magnetic signals that are naturally emitted by the brain. It is widely used to study sensory processing, memory encoding, language, and development among other topics. In clinical neuroscience, it is also used to investigate autism spectrum disorders, movement disorders, and epilepsy [3]. Common uses of MEG are the localization of epileptic foci and presurgical planning via mapping of eloquent areas of the brain i.e. areas that directly control function [6].

The magnitude of magnetic signals measured extracranially is in the order of femtoteslas ($\sim 10^{-15}$ T) which is ten to one hundred million times less than the static magnetic field of the earth [3]. Hence, for MEG devices to detect them, they are most commonly equipped with highly sensitive sensors known as superconducting quantum interference devices (SQUIDs) [6]. SQUIDS operate when cooled below a certain temperature known as the critical temperature (T_c). Commercially available (conventional) MEG devices generally use low critical temperature superconductors (low-T_c SQUIDs). There are also current efforts to develop on-scalp MEG systems that use high critical temperature superconductors (high-T_c SQUIDs) [6]. High-T_c SQUIDs have higher operating temperatures ($\sim$ 77 K) than low-T_c SQUIDs ($\sim$ 4.2 K) and thus require less thermal insulation; this allows the sensors to be placed at a closer proximity to the scalp i.e. reducing the distance from 20 millimeters (mm) down to 1 mm. This allows better capturing of the neuromagnetic signals detectable outside the head and may potentially provide higher spatial resolution [6].

MEG offers several advantages over other imaging methods [3]. One advantage is that it provides a relatively high (sub-millisecond) temporal resolution and a fair spatial resolution. Also, it is considered as a safe and non-invasive method for clinical use; it is a passive recording technique that does not involve the application of external magnetic fields as in Magnetic Resonance Imaging (MRI) and signals are captured outside the head. Additionally, it does not require the use of radioactive substances unlike other imaging modalities such as Single Photon Emission Computed Tomography (SPECT) and Positron Emission Tomography (PET). Furthermore, MEG equipment is considered a more comfortable option when compared to other imaging techniques such as MRI as the patient's posture during recording sessions is flexible; one may either lie down or sit upright. Also, the equipment and setup is generally calm and almost never triggers claustrophobia, anxiety, or stress in patients. Therefore, MEG may be used independently or in combination with other techniques to deepen the understanding of neural activity in the brain.

Despite its advantages, MEG imaging also has its limitations [3]. First, the complexity of its sensing technology and its maintenance impose high capital and operational costs. However, there are ongoing efforts to design more cost-effective

solutions. Also, as magnetic signals from the brain have very small magnitudes, interference may easily arise from electromagnetic noise sources such as electrically powered instruments or moving metal objects. Therefore, MEG recording must be done in a magnetically shielded room which adds to the cost and the difficulty of clinical placement. From another perspective, signals obtained from MEG imaging are rich and complex. Despite the availability of specialized software packages, analysis of MEG data remains a challenge and requires specialized knowledge to extract information that is useful in clinical settings. Furthermore, large datasets require long processing times. Such factors contribute to the limited adoption of MEG.

1.3 Time-Frequency Signal Analysis

Time-frequency (TF) signal analysis refers to the analysis of signals in both time and frequency domains simultaneously using different time-frequency representations. This is particularly important for the study of signals with time-varying frequency content such as those arising from the human brain. These signals are most adequately represented by a TF distribution that reflects how spectral density changes in time [4]. From this, the change in power may be visualized to study the brain's response to various stimuli.

In this section a few standard TF analysis techniques are introduced briefly followed by a more detailed description of a methodology known as Matching Pursuit, which is the technique under investigation herein.

1.3.1 Standard Techniques

Several techniques are used to study and analyze MEG signals. Here, a brief summary of some common standard techniques are presented and the advantages and disadvantages of each are highlighted.

First, the Fourier Transform (FT) [13] decomposes a signal to a linear combination of sinusoidal functions (sines and cosines) at different frequencies; these are known as basis functions. FT is the inner product [14] (see Appendix A.1.1) of a signal with a complex exponential and the magnitude of the inner product at each frequency represents the relative contribution of that frequency to the signal. The energy of the signal is fully preserved after the transform based on Parseval's theorem [15] (see Appendix A.1.2). FT captures the dominant frequency components of a signal, but, as it is a computation of an overall amplitude and phase by integration over the signal duration, it does not reflect how they may change over time and this provides a poor representation of signals well-localized in time [5].

Second, to address the issue of studying the spectral content of a signal as a function of time, the Short-Time Fourier Transform (STFT) may be used. This method decomposes a signal into short time segments equal in size by multiplying it with translated versions of a window function (function that is zero-valued outside of

a chosen interval). Afterwards, Fourier analysis is performed on each segment separately. As the energy of the STFT of the signal is the product of the energies of the signal and the window function, energy conservation is maintained if the energy of the window function is equal to one; this is done using normalization. However, the width of the window affects the time–frequency resolution of the output; reducing the width (time duration) of the window improves the time resolution but leads to a degradation of frequency resolution, and vice versa. Also, the energy of the basis function is not restricted to the time-frequency space that is outlined based on the choice of window function used. Therefore, some of the energy spreads beyond that space causing spectral leakage; this requires the use of different window functions to fulfill different spectral leakage and resolution constraints. In general, most of the frequently used window functions have good spectral concentration; so the main factor affecting the resolution is the width of the window [5].

Third, in the Multitaper (MT) method, a signal is convolved - i.e multiplied in frequency domain - with multiple sliding window functions, each known as a taper; multiple tapers are used per each time window. Then, the energy is calculated for each tapered segment and the energy estimates for each window are averaged. This method reduces the variance across repeated measurements and improves the signal-to-noise ratio (SNR) especially when a large number of measurements is not available. The width of the window may be fixed or variable with changes in frequency values. The tapers are designed to prevent power leakage between neighbouring frequencies; this gives them good frequency specificity. They are also orthogonal to each other, so each gives an independent estimate of the inner product for each time window; this makes MT more reliable for noisy data. However, multitapers are not very sensitive to low-amplitude signals as they are designed to detect non-stationary signals of large-amplitude transients. Additionally, the width of the window function is constant across frequencies just as in a Fourier transform and MT breaks down the TF space into tiles of the same shape. This means that the selected window width determines the resolution achieved; wide windows provide high spectral resolution but at the expense of temporal resolution and vice versa. Therefore, the MT method cannot properly capture both transient and rhythmic components of signals at once [5][16][17].

Fourth is the Wavelet Transform (WT) method. The WT method uses TF tiles of different widths and heights to construct the spectrum of a signal. The basis functions used are scaled and translated versions of a single function known as the mother wavelet. A wavelet is a function that has zero average, unity-normalized energy, and is sufficiently well-localized in time. Due to its properties, a wavelet acts as a bandpass filter and its bandwidth is determined by the scaling factor; for lower scaling values, the filter has larger bandwidths and vice versa. This maintains the proportion between temporal width and frequency bandwidth for all frequencies. In other words, the window width decreases with the increase in frequency values as the frequency is inversely proportional to time. The result is having a better frequency resolution at lower frequencies and good time resolu-

tion at higher frequencies. This approach is therefore advantageous if the signal being studied has transients at higher frequencies and sustained oscillations at lower frequencies. Wavelets also provide more sensitive detection of lower amplitude signals. However, although the TF space is broken down into tiles of different sizes, their position is fixed with respect to frequency values. Therefore, transient activity at low frequencies or rhythmic activity at high frequencies are not well represented [5][16].

As discussed above, each of the methods presented so far has its advantages and disadvantages. Yet, they suffer from the difficulty of capturing both transient and rhythmic components of signals simultaneously. Also, improving one resolution dimension, where applicable, results in the degradation of the other. Figure 2 illustrates some examples of how these standard methods break down the TF plane when applied to signals.The selection of a method is dictated by the nature of the signal and the desirable target resolution. When both time and frequency resolutions are of interest, common workarounds involve applying multiple techniques or performing analysis using one technique but multiple times each with a different window, where applicable, for the analysis of a single signal. This all requires additional effort and time and does not facilitate studying the complete frequency content of the signal. This leads to the last method, Matching Pursuit, which will be described in more depth in the following subsection.

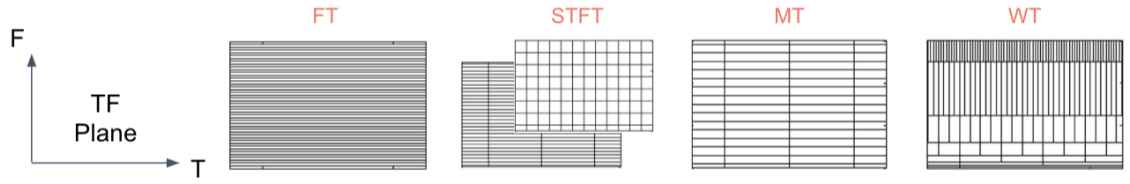

Figure 2: TF plane decomposition examples from standard analysis methods. Left to right: 1) FT decomposes the TF plane into frequency components only and thus does not provide good representation for signals well-localized in time. 2) STFT decomposes the TF plane into identical blocks (top: small time window, bottom: large time window). 3) MT also decomposes into identical blocks with the dimensions depending on the time window used. 4) WT decomposes the TF plane in a frequency scaled manner with the window size decreasing as frequency increases. However, each tile shape and size is fixed with respect to the frequency axis. This makes it difficult to capture frequency content of waveforms whose Fourier transforms are well localized at high frequencies and also signal content that is well-localized in time at low frequencies. In summary, in the STFT, MT and WT methods, improvement in time resolution results in degradation of frequency resolution and vice versa. Image adapted from Chandran et al., 2016 [5].

As the details of the techniques above are beyond the scope of this project, a more detailed comparison may be found in the works of Chandran et al., 2016 [5] and van Vugt et al., 2007 [16]. This report focuses mainly on the application of the Matching Pursuit method for the analysis of MEG signals.

1.3.2 Matching Pursuit

This project focuses on the application of an algorithm known as Matching Pursuit (MP) for the analysis of gamma oscillations recorded from the brain, which

include both transient and rhythmic components. Therefore, this subsection has been dedicated to a more elaborate presentation of this technique, its advantages over the standard methods summarized above, in addition to its limitations.

MP [5][18] is an iterative greedy algorithm that decomposes a signal into a linear expansion of waveforms or functions, known as time-frequency atoms, whose TF properties are adapted to its local structures. It is 'greedy' in the sense that in each iteration, it makes a locally-optimal choice that seems to be the best at that step with the hope that it would lead to a globally-optimal solution. The locally-optimal choice is the selection of an atom that best approximates part of the signal (local properties) at a given iteration. The atoms are selected from an over-complete (redundant) dictionary obtained by shifting, scaling, and modulating a single window function $g(t) \in L^2(R)$. g(t) is continuously differentiable and normalized to unity i.e. $||g(t)|| = 1$ to ensure energy conservation by enforcing unity-valued energy. $L^2(R)$ is the Hilbert space (see Appendix A.1.3) of complex-valued functions [18][19]. The scaling, translation, and modulation of a function is reflected in the simple modifications of the selected atom indices within the dictionary.

The atoms are well-localized in time and frequency. However, they vary in time and frequency resolutions; a delta function provides high time resolution but no frequency information, a Fourier decomposition provides high frequency (spectral) resolution but no temporal information, and other functions form a collection of intermediate TF-resolution combinations (figure 3). This enables the computation of more adaptive TF signal representations of a signal when compared to the standard methods described above.

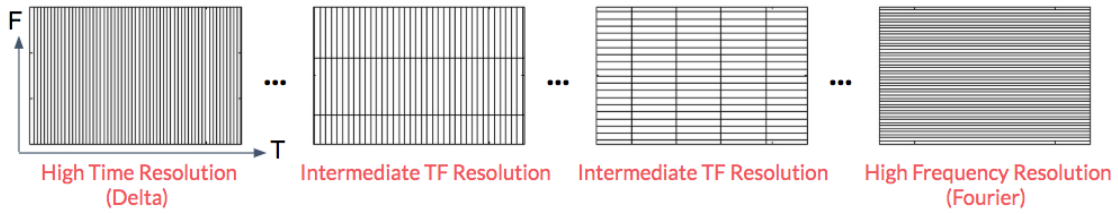

Figure 3: Time-frequency plane decomposition examples from atoms in an MP dictionary. Left: delta function (time resolution only). Right: Fourier transform (frequency resolution only). Center: different time-frequency resolution combinations. Image adapted from Chandran et al., 2016 [5].

The choice of library should be based on the nature of the signal being analyzed. Depending on this choice, decomposition may result in very different properties. This project experiments with two types of dictionaries: dyadic [18] and stochastic [20]. Both dictionaries are based on Gabor functions (see Appendix A.2), which are time-frequency atoms derived from a Gaussian window. Gabor dictionaries are suitable for the analysis of the gamma rhythm as its center frequency does not vary with time; it is slightly high at the onset of a stimulus-triggered response but then quickly stabilizes to a steady value [20]. Discrete delta and Fourier bases are also added to the dictionaries to cover edge cases of

the TF plane i.e. the highest temporal resolution and the highest frequency resolution respectively. To understand the key difference between the two dictionaries, one must return to the scale, time shift, and frequency modulation parameters that are used to generate each over-complete dictionary. In the case of a dyadic dictionary [20], these parameters are sampled by changing the scale s of the atom in powers of two. The sampling is governed by an integer parameter known as the Octave v. The scale s, which reflects an atom's width in time, is obtained from the dyadic sequence $s = 2^v, 0 \leq v \leq L$, where $L = log_2 N$ is an integer such that the signal size N becomes limited to $N = 2^L$. The other parameters corresponding to an atom's position in time and frequency are usually sampled for each octave using an interval of $s = 2^v$. For a signal of length N, the number of atoms in the dyadic dictionary would be in the order of $O(NlogN)$ atoms.

For a stochastic dictionary [21] on the other hand, the parameters are sampled uniformly over a large range. In this case, the number of atoms in the dictionary (size of dictionary) is independent of N because the parametric space may be broken down into arbitrary small-sized divisions or blocks, from which atoms are selected. This allows deriving dictionaries of various sizes for a given signal. Furthermore, in a stochastic dictionary, the parameters of the atoms are randomized before each decomposition to reduce bias that may result from sub-sampling the parameter space.

To understand how the method works [5][22][18], a high-level overview of the steps involved in the MP technique are described next. The goal is to compute a linear expansion of a function f over a set of atoms from a dictionary that match its inner structures in the best possible way using successive approximations of f. At the beginning, MP sets the value of the decomposed signal to zero. A residue term is also defined to represent the error computed after approximation of part of the signal; this is given by the difference between the signal and the approximation. Hence, at the beginning, the residue is set to the value of the signal itself as the approximated signal is zero. Each iteration involves two steps: atom selection and residue update. The selection step picks up the atom which has the highest correlation or the with the current residue or in other words the atom that best approximates a part of the signal. Sometimes, it is only possible to find an atom that is almost the best based on an optimality factor (see Appendix A.2.1). The matching is done by computing the inner product between the residue and all the atoms in a given dictionary and evaluating their coherence with the signal structure (current residue). The coherence measure is based on finding atoms that have a higher than average correlation with the residue. From the set of coherent atoms, the one that returns the highest value of the inner product is selected. If a structure does not correlate well with any particular atom in the dictionary, it is broken down into several segments for which matching atoms are sought and so on. The correlation is determined using a predefined correlation ratio (see Appendix A.2.1). The signal approximation is given by multiplying the selected atom by its corresponding inner product with the residue. The update step modifies the residue value by subtracting the signal approximation (matched part)

from the signal. The procedure is repeated over many iterations and the residue after the n^{th} iteration represents the difference between the signal and the total signal approximation up to the n^{th} iteration.

The atoms are not orthogonal to one another, however, the residue computed after an iteration is orthogonal to the atom selected at that iteration; this ensures that the energy of the residue approaches zero as the number of iterations approaches infinity and that the energy of the decomposed signal is equal to the sum of the square of the inner product terms i.e. energy conservation is achieved. The iterations end once specific criteria (e.g. approximation precision) are met or once the maximum number of iterations is reached (if specified as done in this project). In this case, the total number of atoms selected to represent the signal at the end depends on the number of iterations executed by the MP algorithm; when the number of iterations is high, MP ends up choosing atoms with very small magnitudes over all frequency ranges [5][22][18].

The MP process is basically decomposing a signal into smaller segments and reconstructing it using the best matching atoms from the dictionary being used. The search over a dictionary identifies the approximate scale, time, and frequency localization of the main signal structures from a subset of atoms in the dictionary. Then, these values are refined using Newton's iterative optimization method to obtain the TF parameters that best match the signal components. The properties of the signal components are given by the scale, time, frequency, and phase indices of the chosen atoms. The dictionary can be thought of as a box that is full of TF tiles of different sizes and rectangular shapes just like a large variety of puzzle pieces; the algorithm only selects the puzzle pieces (atoms in this case) that would best approximate the target image (the decomposed signal in this analogy). By the end of the process, the TF space is covered with the custom selected TF tiles based on the properties of the signal being analyzed. A simplified summary of the theory behind matching pursuit along with an illustrative flowchart are available in Appendix A.2 [18].

After the decomposition of the signal to atoms a TF power distribution is generated for each tile (selected atom) and the signal's TF energy distribution is obtained by summing the Wigner distributions of the selected atoms. This project uses the Wigner-Ville distribution (WVD) [5][23]. The WVD provides a generalized spectrum for time-varying spectral analysis which plays a major role in understanding the properties of non-stationary signals [24]. The conventional WVD formula contains both cross-terms (interference terms) and self-terms (independent terms). However, since MP decomposition conserves the energy of the signal, cross-terms are ignored; the self-terms fully represent the energy of the original signal. Therefore, the TF distribution generated for each TF tile does not include interference terms from neighbouring tiles and provides a clear visualization in the TF plane [5][18][21]. A brief description of the WVD implementation used is available in Appendix A.2.2.

MP offers several advantages with respect to TF resolution and adaptivity to transient structures when compared to the techniques discussed above [5]. The method allows breaking down the signal's TF space into custom shaped tiles that better represent the signal when compared to tiles of fixed width or tiles that have frequency dependent width values as seen in the standard methods. Also, in MP, the tiles can be located at any position on the TF plane. Furthermore, in standard methods a fixed set of tiles is used for all stimulus repetitions. When averaged across repetitions, only the values within each tile are averaged. However, in MP, as each repetition would result in a different set of tiles, averaging across repetitions also averages out the shapes of the tiles. Finally, in methods that involve windowing, the window width and its temporal overlap - which are fixed parameters - determine smoothing. In MP, this smoothing is also tailored to the nature of the signal. Therefore, due to its adaptive nature, MP can capture and visualize both transient and rhythmic components of signals simultaneously. MP is mainly distinguished by its ability to capture sharp transients in signals which is usually a difficult endeavour when using traditional analysis methods.

However, despite MP's advantages, the method has some limitations [5][20]. First, the dictionary should be chosen to suit the signal being studied, otherwise the quality of analysis may not be optimal. Also, since a selection of different atoms is used for signal decomposition, it is difficult to perform phase coupling comparisons in signals such as phase amplitude coupling (PAC) that studies how the phase of the slower (lower frequency) oscillation drives the power of the coupled faster (higher frequency) oscillation.

From another perspective, the signal is checked against a large number of atoms in the dictionary to obtain the best match in a multitude of iterations; this process requires time and therefore results in performance limitations especially when multiple trials and multiple MEG channels (large datasets) are involved in the analysis. Also, with MP being a greedy algorithm, if a wrong atom is picked up in some iteration, the algorithm tries to correct this in following iterations, which would further increase the execution time.

One final important point to keep in mind is the minimum signal length needed for MP analysis. In most decomposition techniques, artifacts arise around the boundaries (starting and ending time points) of the segment of the signal being analyzed. This is due to the periodicity assumption of the discrete Fourier transform (DFT) [25], which is often used for signal analysis. In window-based methods, the effects of these artifacts are minimized when multiplying by a window such that the edge values of the signal approach zero. The MP decomposition, however, does not use any explicit windows. To avoid the appearance of such artifacts in intervals of interest, it is recommended to use a signal that has a much greater length than the duration of interest e.g. at least three times longer and then investigate only the middle part of the output. As expected, this would increase the analysis time and also require additional computational resources.

The scope of this report is mainly concerned with the application of the MP method for MEG analysis. A complete description of the MP algorithm and the mathematical foundation behind it is provided by Mallat and Zhang 1993 [18].

1.4 Aims and Objectives

When applied to the analysis of EEG recordings from monkeys using intracranial electrodes [20][5][26], the Matching Pursuit algorithm provided enhanced time and spectral resolutions. This project aims to apply the MP technique to investigate whether similar results may be reproduced when analyzing MEG recordings from human subjects. The signals analyzed herein represent gamma activity induced in the visual cortex of the human brain in response to visual stimuli.

Based on the outcome of the exploratory experiment above, the project also aims to test the ability of conventional and on-scalp MEG systems to detect different types of gamma activity and thereby provide different information upon analysis. Finally, and with regard to clinical diagnostics and elucidation of neurofunctional deficits, the project also seeks to investigate whether or not the method would reveal biomarkers that may be used to distinguish between groups of human subjects with and without autism spectrum disorder (ASD) based on the different characteristics of the analyzed gamma activity.

2 Methods

This section covers the methods used throughout the project. This includes the literature review, software implementation, and data analysis steps.

2.1 Literature Review

Literature review was carried out to support the different aspects of the project such as background information, relevant methods, and software resources. This includes books, scientific papers, and online resources found using Google Web Search [27], Google Scholar [28], and Chalmers University of Technology's online library [29] with access to various scientific publishing sources.

The project relied mainly on the work described by Chandran et al., 2016 [5] and Chandran Ks et al., 2017 [20] on the application of MP for the study of EEG recording from monkeys. This in turn lead to the papers by Mallat and Zhang 1993 [18] and Durka, Piotr J., Dobieslaw Ircha, and Katarzyna J. Blinowska [21] for details on the different implementations. Other sources were also referenced for additional details and to support the introduction and background information.

2.2 Software Implementation

The software used to produce the results is a combination of adapted code based on relevant papers and supplementary functionality that was added to accommodate the desired data analysis process. The code is fully commented and available for download at the link below:

https://github.com/tgoudian/meg_mp

The following is an overview of the key software development activities that were carried out using MATLAB R2018b [30].

2.2.1 MP Algorithm

Two implementations of the MP time-frequency analysis algorithm were modified and transformed into a modular format to allow users to switch between them in a simple manner. First, an MP implementation using a dyadic dictionary developed by Chandran et al., 2016 [5][31]. Second, an MP implementation using a stochastic dictionary as described by Chandran Ks et al., 2017 [20][32]. The theory behind the functionality of the MP algorithm is described in Appendix A.2.

Both implementations involve a combination of C and Matlab source code. An independent copy of the Matlab code was modified for both versions to accommodate the following:

- Support of MEG data input instead of the EEG data format for which the code was originally developed.
- Data reformatting for compatibility with the MP implementations.
- Proper data scaling as MEG data values are in the order of femtotesla.
- Disabling the time wrapping option provided in the dyadic MP implementation [31] to avoid signal duplication at time boundaries.
- Modularity of the code for reuse and easy modification.

2.2.2 Data Analysis Workflow

The data analysis workflow is based on the method used by Orekhova, Elena V., et al. [33] [12] for which sample code was provided by the author. The code was adapted to replace the multitaper TF analysis [34] functionality provided by the FieldTrip toolkit [35] with the MP implementations described above. Additional intermediary prepossessing steps relevant to MEG data formatting based on the type of input and analysis desired were developed. Also, the software was written in a manner that allows compatibility of data structures and workflows and flexibility to allow for the study of multiple subjects, MEG channels, and trials.

2.3 MEG Data

The data used for signal analysis was provided by the project supervisors after removing known sources of noise (e.g. power line interference)and represents MEG recordings from adult subjects who were previously classified as either neurotypical (NT) or diagnosed with autism spectrum disorder (ASD). The term, neurotypical refers to subjects not displaying autistic or other neurologically atypical patterns of thought or behaviour.

The subjects were exposed to visual stimuli to investigate their responses as reflected in gamma waves. Each trial began by displaying a fixation cross that was followed by a circular grating drifting inward for 1.2 to 3 seconds (s) at one of three speeds - slow (1.2°/s), medium (3.6°/s), and fast (6.0°/s) - where each speed value represents a condition. Each participant was requested to press a button to indicate the end of motion. Short animated clips (3-6 s) of cartoon characters were displayed randomly between every 2-5 stimuli triggers to maintain attentiveness and reduce visual fatigue. Each of the 3 stimulus types was repeated for many trials (listed below); those that were contaminated by motion or technical artifacts were excluded from subsequent analysis steps. More details on the experimental setup followed for data acquisition is available in the works of Orekhova, Elena V., et al. [33] [12]. Three MEG datasets were used:

- Test Dataset (90 trials/condition): 2 subjects (one NT and one ASD) for 2 conditions (1:slow, 2:fast) obtained using a low-T_c MEG device.
- Dataset A (500 trials/condition): 3 NT subjects for 2 conditions (1:slow, 2:fast) obtained using both low-T_c and high-T_c MEG devices.
- Dataset B (90 trials/condition): 19 NT and 20 subjects with ASD for 3 conditions (1:slow, 2:medium, 3:fast) using a low-T_c MEG device.

The data files are not made public for privacy and confidentiality purposes. Access to data is subject to written authorization by the project supervisors.

2.4 Data Analysis using a Dyadic Dictionary

Here , the analysis processes that was carried out using a dyadic dictionary are described.

2.4.1 Comparison of Matching Pursuit and Multitaper Methods

At the beginning, a test to compare the output of the MP and MT methods was done as a proof of concept to ensure that the results obtained by Chandran et al., 2016 [5] for EEG data may be replicated for MEG data as well. MT is chosen as an example only to demonstrate the problem faced when using standard techniques;

the propose is not to conduct a comparison with all other methods. The analysis for both techniques was executed on the same dataset (Test Dataset) and settings.

Before running the MP and MT analyses, an additional MT analysis was run using the function ft_freqanalysis from the Fieldtrip toolkit [17]. This was done to determine the channel (sensor) that has the maximum increase in gamma power based on the ratio of post-stimulus and pre-stimulus power for each channel. As the analysis processes are time-consuming, using one channel would be sufficient to run the test. The gamma range used for this step was set to 45-90 Hz.

The script '/matlab/SpectralAnalysis/MT_MP_Comp_MP_Analysis.m' was used to run the MP analysis with the following settings for low-T_c MEG data:

DataSource:	'LTC' (low-T_c MEG data)
MPDic:	'dyadic' (dyadic dictionary)
subtractAvg: [0]	evoked response subtraction disabled
ModeText:'NoSubEvoked'	evoked response subtraction disabled
MPmaxIterations:	500 (Number of MP iterations)
baseline_range:	[-0.8 0] s (Pre-stimilus time range before stimulus trigger at time 0)
post_stimulus_range:	[0.4 1.2] s (post-stimulus time range after stimulus trigger)

The evoked response subtraction was added to ensure that the output reflects the MEG data rather than artifacts that may have been introduced by the method used. This was done by calculating the average of all trials and then subtracting the average values from each trial.

For the MT analysis, the following script was used with the settings below:
'/matlab/SpectralAnalysis/MT_MP_Comp_MT_Analysis.m'

Baseline range:	[-0.8 0] s
Post-stimulus range:	[0.4 1.2] s

The ft_freqanalysis function was used for MT analysis with a fixed window:

cfg.method:	mtmconvol (multitaper TF transform based on multiplication in the frequency domain)
cfg.output:	pow (power-spectra)
cfg.taper:	dpss (discrete prolate spheroidal sequences (Slepian window)
cfg.foi:	[5:1:150] Hz (frequency band of interest)
cfg.toi:	[-1.0:0.01:1.2] s (the time points on which the analysis windows should be centered)
cfg.tapsmofrq:	5 Hz (the amount of spectral smoothing through multitapering. Plus-minus 5 i.e. a 10 Hz box)
cfg.t_ftimwin:	0.4 s (length of time window)

Then ft_freqanalysis was used again for MT analysis with a scaled windows:

cfg.method:	mtmconvol
cfg.output:	pow
cfg.taper:	dpss
cfg.foi:	[5:1:150] Hz
cfg.toi:	[-1.0:0.01:1.2] s
cfg.tapsmofrq:	cfg.foi*0.2 Hz
cfg.t_ftimwin:	5./cfg.foi s

The MT method was run once with a fixed time window (0.4 s) to capture rhythmic components and then another time with a frequency-scaled time window ($window = 5/frequency$) to capture transient components. In the latter mode, the time window decreases in width with increasing frequency. The window used is a Slepian window or Discrete Prolate Spheroidal Sequences (DPSS) [33][12].

For the analysis, the maximum channel and all 3 conditions (1, 2, 3) were used for 2 subjects: one from the NT category and the other diagnosed with ASD. The sampling frequency rate and signal length were given with the data files. Details on the Fieldtrip functions used and their parameters can be found in Fieldtrip's documentation [36] as they are beyond the scope of this project. MT is only introduced here to demonstrate the problem faced with standard techniques and show how MP improves the output.

With regards to the post-stimulus range, the first few hundred milliseconds after stimulus onset are excluded from analysis to avoid response transients. This is particularly important to study the power spectra of the late rhythmic component of the signal. This applies to all MP analysis in this report.

It is important to note that the implementations assume the value of 1 for the MP optimality factor (see Appendix A.2.1) to search the full dictionary [18] and the number of iterations was kept at the default value (500) [5], to ensure that the

approximation captures both high and low magnitude signal components.

2.4.2 Comparison of Low-T_c and High-T_c MEG Systems

This experiment was conducted to compare the information content and quality obtained in data recorded with low-T_c and high-T_c MEG devices.

For this part, the script '/matlab/SpectralAnalysis/MP_RunAnalysis.m' was used with the following settings for low-T_c MEG data:

DataSource:	'LTC' (low-T_c MEG data)
MPDic:	'dyadic' (dyadic dictionary)
MaxChannel:	1 (maximum channel analysis)
EVENTS:	[1,2] (list of events or conditions))
subtractAvg: [0]	evoked response subtraction disabled
ModeText:'NoSubEvoked'	evoked response subtraction disabled
MPmaxIterations:	500 (Number of MP iterations)
baseline_range:	[-0.7 -0.1] s (Pre-stimilus time range before stimulus trigger at time 0)
post_stimulus_range:	[0.4 1] s (post-stimulus time range after stimulus trigger)

The same setting were used for high-T_c MEG data except DataSource which was set to 'HTC' to handle the data structure difference.

The analysis was conducted on Dataset A for the channel with maximum stimulation-related power increase only; this was sufficient to investigate the quality of the MP algorithm output as running MP on all channels would be time consuming. The maximum channel was already predetermined and provided in the dataset. The sampling frequency rate and signal length were given with the dataset.

As the dyadic dictionary performs sampling in powers of 2, it only works for signals that have a length (number of time points) that is a power of 2. Unfortunately, the data available did not satisfy this condition and part of it was discarded from the end (latest time points). However, it is not recommended to discard data. Instead, a longer signal (with a length of the next power of 2) should be acquired from recordings. The datasets used were sufficient for the project at hand but it is important to note that the high-T_c dataset was longer than the low-T_c dataset.

Before proceeding with other experiments, this test was repeated with subtractAvg:[1] and modeText:'SubEvoked' i.e. with evoked response subtraction enabled.

2.4.3 Group Comparison of NT and ASD Subjects

This experiment was performed to investigate the possibility of identifying features in MEG data that may help in differentiating between NT and ASD subjects.

The scripts '/matlab/SpectralAnalysis/MP_RunAnalysis_Groups.m' and then '/matlab/SpectralAnalysis/MP_PlotGroupAvg.m' were used with the settings below:

DataSource:	'MaxSenVox' (sensor with maximal increase of gamma power)
MPDic:	'dyadic' (dyadic dictionary)
EVENTS:	[1,2,3] (list of events or conditions))
subtractAvg: [0]	evoked response subtraction disabled
ModeText:'NoSubEvoked'	evoked response subtraction disabled
MPmaxIterations:	500 (Number of MP iterations)
baseline_range:	[-0.7 -0.1] s (Pre-stimilus time range before stimulus trigger at time 0)
post_stimulus_range:	[0.4 1] s (post-stimulus time range after stimulus trigger)

The analysis was conducted on Dataset B for the sensor with maximal increase of gamma power (40-90 Hz) for data recorded from a low-T_c MEG device only. The sampling frequency and signal length were given with the data files. After the MP output was obtained, the average power was calculated for each group-condition combination and then the change in power relative to the baseline (pre-stimulus state) was calculated to produce plots for the comparison of gamma responses between groups for each condition.

2.5 Comparison of Dyadic and Stochastic Dictionaries

Finally, a test was performed to evaluate whether using a more extensive stochastic dictionary would result in significant improvements in analysis quality when compared to a dyadic dictionary.

Here, the script '/matlab/SpectralAnalysis/MP_RunAnalysis.m' was used again with the following settings for low-T_c MEG data (Dataset A):

DataSource:	'LTC' (low-T_c MEG data)
MaxChannel:	1 (maximum channel analysis)
EVENTS:	[1,2] (list of events or conditions))
subtractAvg: [0]	evoked response subtraction disabled
ModeText:'NoSubEvoked'	evoked response subtraction disabled
MPmaxIterations:	500 (Number of MP iterations)
baseline_range:	[-0.7 -0.1] s (Pre-stimulus time range before stimulus trigger at time 0)
post_stimulus_range:	[0.4 1] s (post-stimulus time range after stimulus trigger)
norm_factor:	10^{12} (Normalization factor to accommodate femtotesla values)
adaptiveDictionaryParam (ADP):	0.9 (adaptive dictionary parameter 0-1, used to select subset of dictionary for faster execution, default 0.9) $subsetSize = (1 - ADP) \times 100\%$
dictionarySize:	2500000 atoms (dictionary size)

The script was run once with MPDic:'dyadic' and then again with MPDic:'stochastic' for the same NT subject low-T_c data from the comparison of low-T_c and high-T_c MEG systems above.

In the dyadic implementation, cosine-modulated Gabor functions were used [5], while sine-modulated Gabor functions were used in the stochastic case [21]. Also, in the stochastic version, a large dictionary size (2500000) was used to ensure that results were not biased by insufficient sampling of the parameter space (determined experimentally by Chandran Ks et al., 2017 [20]). The adaptiveDictionaryParam was also kept at the default value as used by Durka et al. 2001 [21][37].

2.6 Plot Generation

Two types of plots were used to illustrate the results. The first, a TF power plot reflecting the change in power along the time and frequency axes. The second displays the power spectra (average post-stimulus power change versus frequency).

For the analysis steps above, the change in power is calculated for each subject, one channel, and one condition at a time for all trials. To visualize these event-related power changes, normalization with respect to the baseline (pre-stimulus) interval is performed. First, the output of MP is averaged over all trials to produce the mean power matrix ($MeanP$). Then, the change in power between $MeanP$ and the time average of baseline values ($BaselineAvg$) is computed.

For TF power plots, the change is calculated using a logarithmic scale in decibels (dB) based on the following formulae:

$$BaselineAvg = Avg[log(BaselineMeanP)] \tag{1}$$

$$PowerChange = 10 * [log(MeanP) - BaselineAvg^*] \tag{2}$$

MeanP is a 2D power matrix with frequencies as rows and time points as columns, *BaselineMeanP* is the same but for the baseline time range only, *BaselineAvg* is a column vector representing the average of power values over the baseline time range, and $BaselineAvg^*$ is a matrix with the *BaselineAvg* column vector repeated for the total number of time points; i.e. the baseline average value for each frequency is subtracted from corresponding entries in the mean *MeanP*. The output matrix *PowerChange* is plotted. The logarithmic scale was used because otherwise the power at higher frequency values would be difficult to capture especially since it is usually only a small fraction of the signal's total power.

Applying the same logic above for power spectra plots, the relative change with respect to the baseline interval is calculated as a ratio from raw values as follows:

$$BaselineAvg = Avg(BaselineMeanP) \tag{3}$$

$$PowerChangeMatrix = \frac{(MeanP - BaselineAvg^*)}{BaselineAvg^*} \tag{4}$$

Then, from the *PowerChange* matrix, the time average of the post-stimulus change in power is calculated and plotted against frequency values.

3 Results

This section presents the results of the analyses described in the methods section. MP is explored in attempt to achieve better time and frequency resolutions.

3.1 Data Analysis using a Dyadic Dictionary

First, the results of dyadic dictionary MP analysis are described in this subsection.

3.1.1 Comparison of Matching Pursuit and Multitaper methods

The results of applying the MT and MP methods to MEG data from 2 adult subjects are visualized for comparison in figures 4 and 5. Only one condition is included as the others demonstrate similar results and my be accessed at:

https://github.com/tgoudian/meg_mp/tree/master/Plots/MP_vs_MT

The plots represent the change in power in relation to the onset of the stimulus (change in power between post-stimulus and average baseline values). MT best captures rhythmic components of the signal with a fixed window while transient components are better represented using a scaled window. MP, on the other hand, demonstrates an enhanced representation of both components simultaneously.

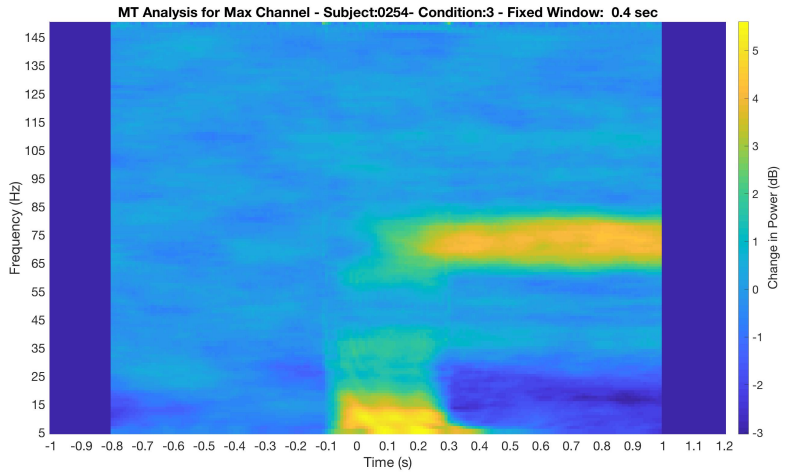

(a)

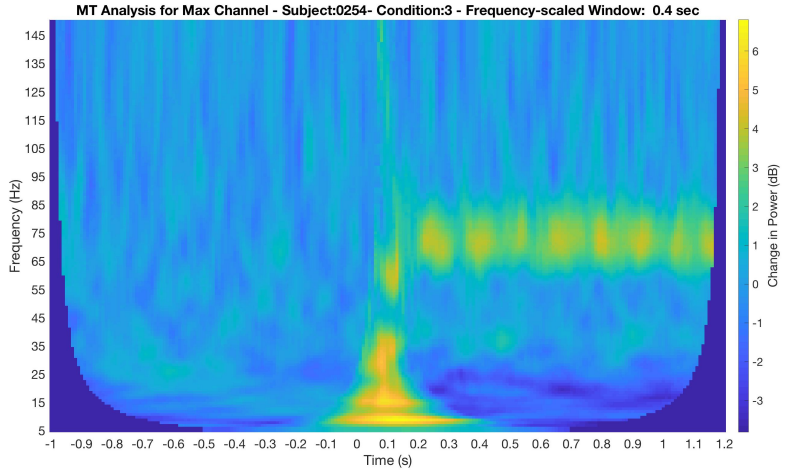

(b)

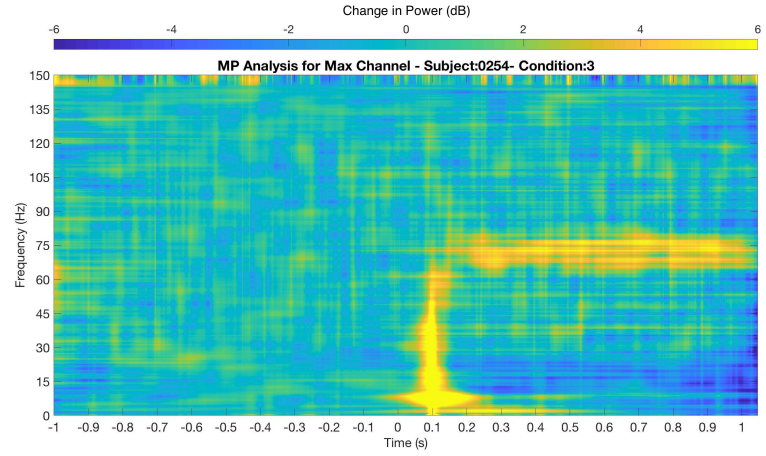

(c)

Figure 4: TF power plots for ASD subject and condition 3 (fast stimulus). Plot (a) is the output of the MT method with a fixed window (0.4s). Plot (b) is the output of the MT method with a frequency-scaled window ($window = 5/frequency$). Plot (c) is the output of the MP method. The color gradient shows the change in power; blue indicates power suppression and yellow indicates increase in power. The plots illustrate the enhanced ability of MP to capture both transient and rhythmic components of the signal concurrently.

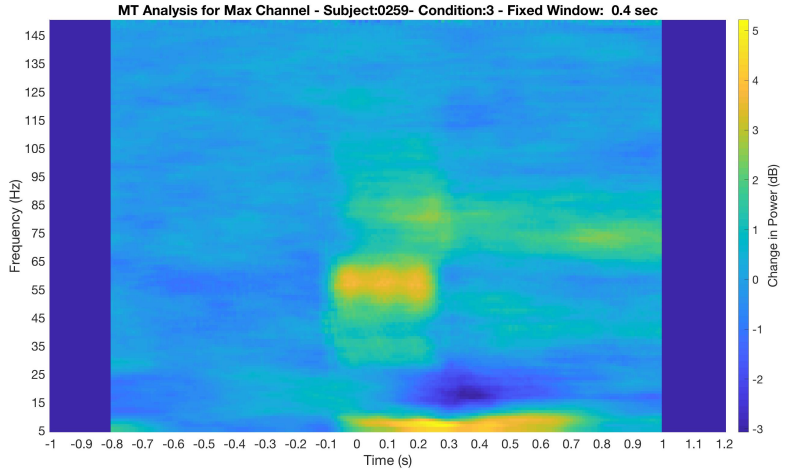

(a)

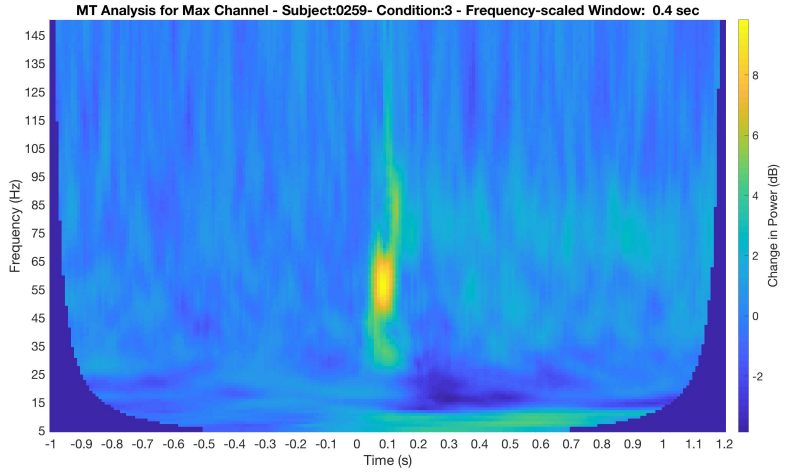

(b)

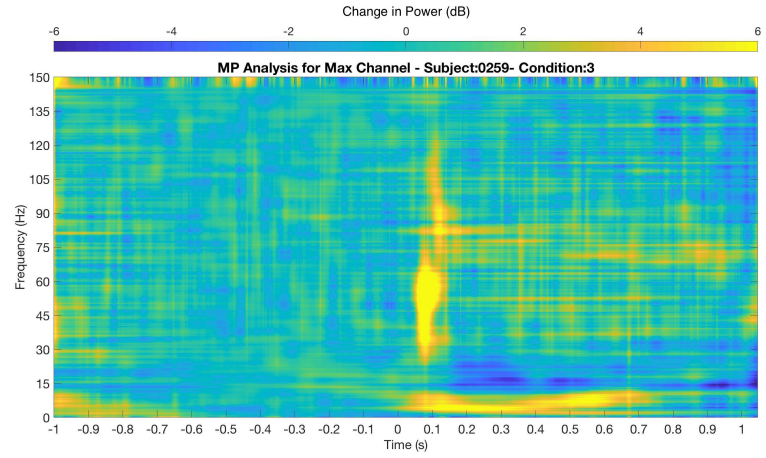

(c)

Figure 5: TF power plots for NT subject and condition 3 (fast stimulus). Plot (a) is the output of the MT method with a fixed window (0.4s). Plot (b) is the output of the MT method with a frequency-scaled window ($window = 5/frequency$). Plot (c) is the output of the MP method. The plots illustrate the enhanced ability of MP to capture both transient and rhythmic components of the signal concurrently.

3.1.2 Comparison of Low-T_c and High-T_c MEG Systems

The results of analyzing MEG data recorded from both low-T_c and high-T_c MEG are shown for comparison in figures 6, 7, and 8. Plots for one subject (NT) were chosen to demonstrate the results as the high-T_c data obtained from the two other subjects had a low signal-to-noise ratio due to environmental noise during recording. All plots may be accessed at:

https://github.com/tgoudian/meg_mp/tree/master/Plots/HTC_vs_LTC

For each of the three figures, plot (a) represents data obtained from a low-T_c MEG device and plot (b) represents that from a high-T_c MEG device. Figures 6 and 7 show the TF power plots for condition 1 and 2 respectively. It is important to note that timeline for high-T_c plots is shorter than the corresponding low-T_c plots. As explained in the methods section, the dyadic dictionary uses sampling in powers of 2. Since the high-T_c dataset was longer than the low-T_c dataset, more data points were discarded from the end of the high-T_c signal. This is due to the increase in the distance between the power of two values as the exponent becomes greater. However, the plots are sufficient to demonstrate the differences between the two devices. Figure 8 displays the power spectra for both conditions.

The plots reveal some evident differences between the low-T_c MEG data and the high-T_c MEG data. From, plot (b) in figures 7 and 8, increased power change during stimulation is observed in the lower gamma region with a peak slightly above 30 Hz. This is seen in the high-T_c but not in the low-T_c recording.

On the other hand, the high-T_c plot does not capture the early gamma transient component that is seen in the low-T_c plots despite MP's sensitivity to transient components and its detection of power suppression in data from both devices. The same result (not shown) was obtained when the MT method was applied to the same dataset by the project supervisor [38]. This could be attributed to high levels of noise in the high-T_c sensors.

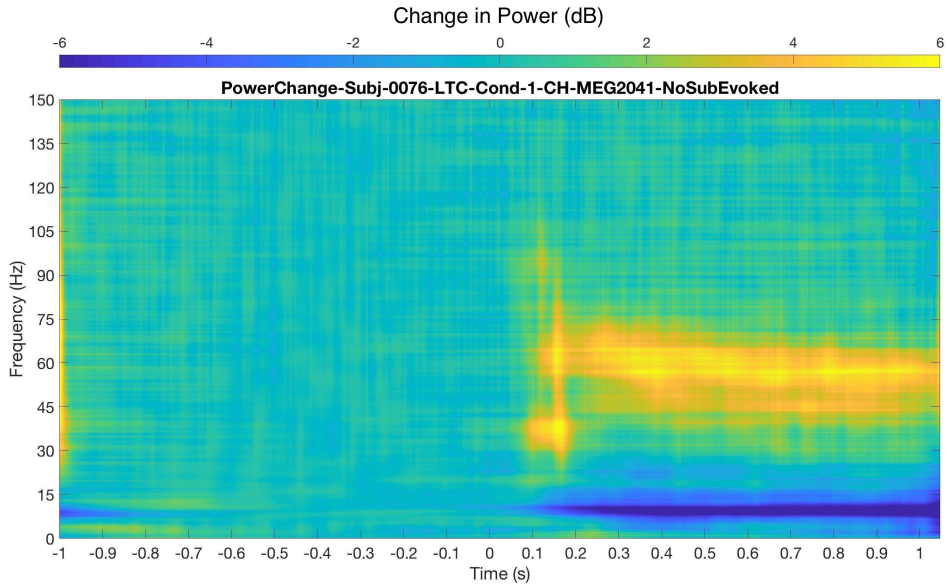

(a)

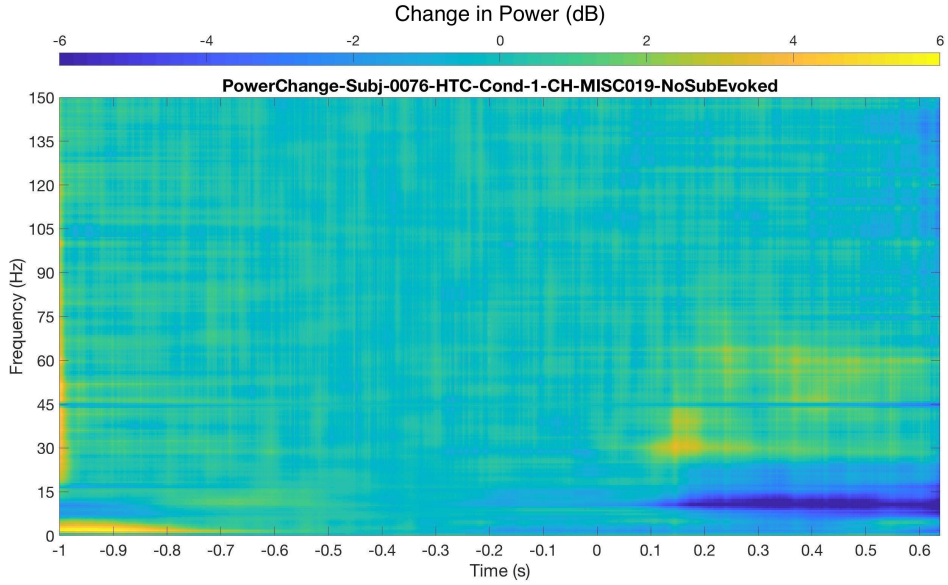

(b)

Figure 6: TF power plots for NT subject and condition 1 (slow stimulus). (a) Low-T_c MEG data (b) High-T_c MEG data. The color gradient shows the change in power; blue indicates power suppression and yellow indicates increase in power. Unlike the low-T_c plot, the high-T_c plot only reveals some 'late' sustained gamma activity and the early transient response is entirely absent. This is most probably due to the high level of noise in the high-T_c sensor.

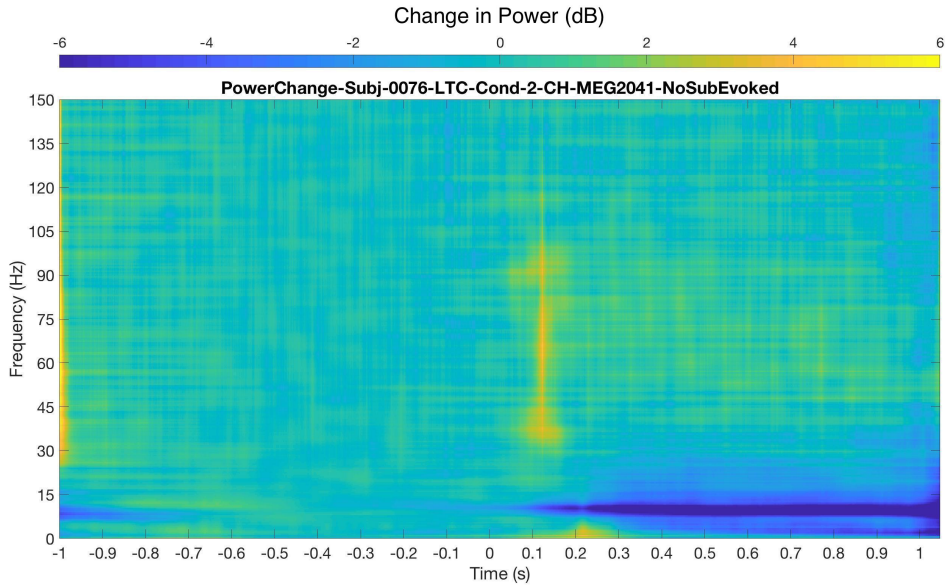

(a)

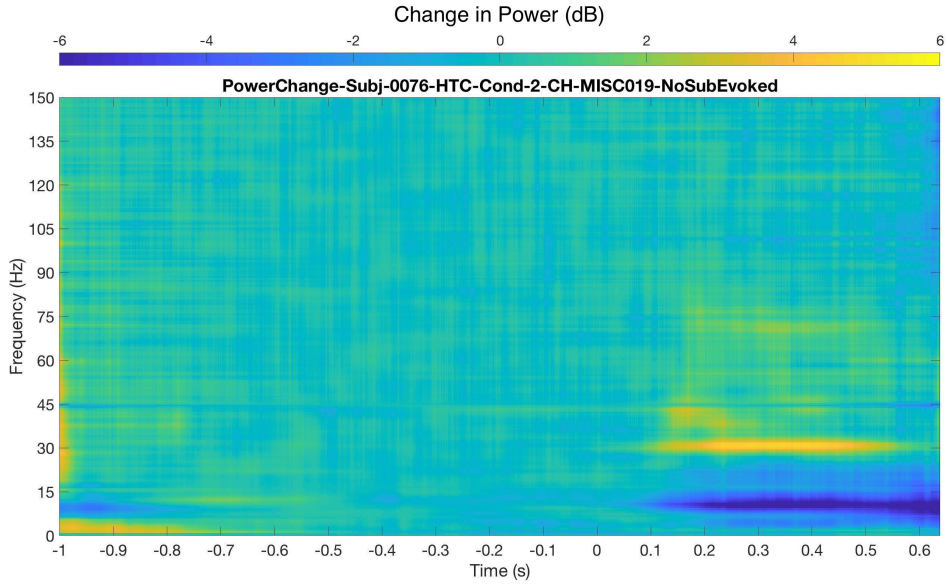

(b)

Figure 7: TF power plots for NT subject and condition 2. (a) Low-T_c MEG data (b) High-T_c MEG data. The high-T_c plot reveals some 'late' sustained gamma activity at around 30Hz, which is not seen in the low-T_c plot. The early transient response is also entirely absent in high-T_c plot; this is most probably due to the high level of noise in the high-T_c sensor.

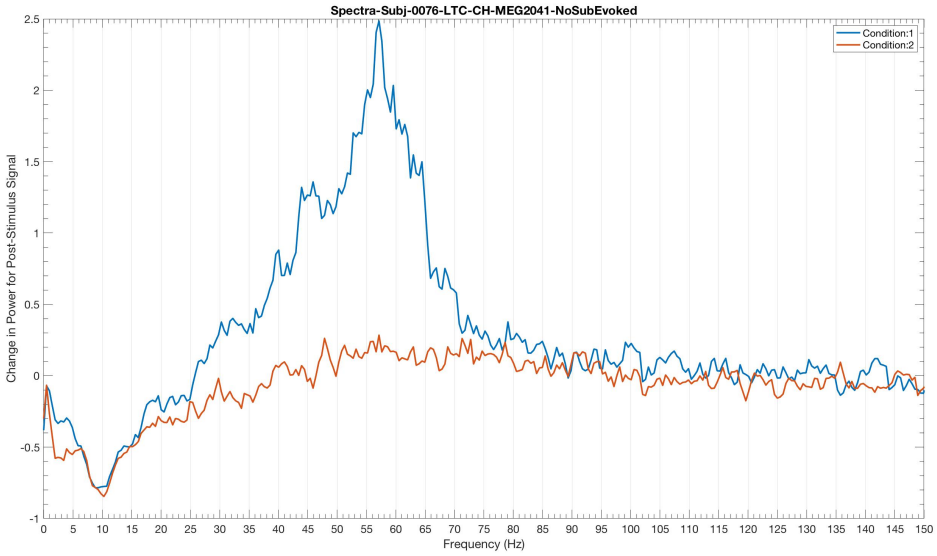

(a)

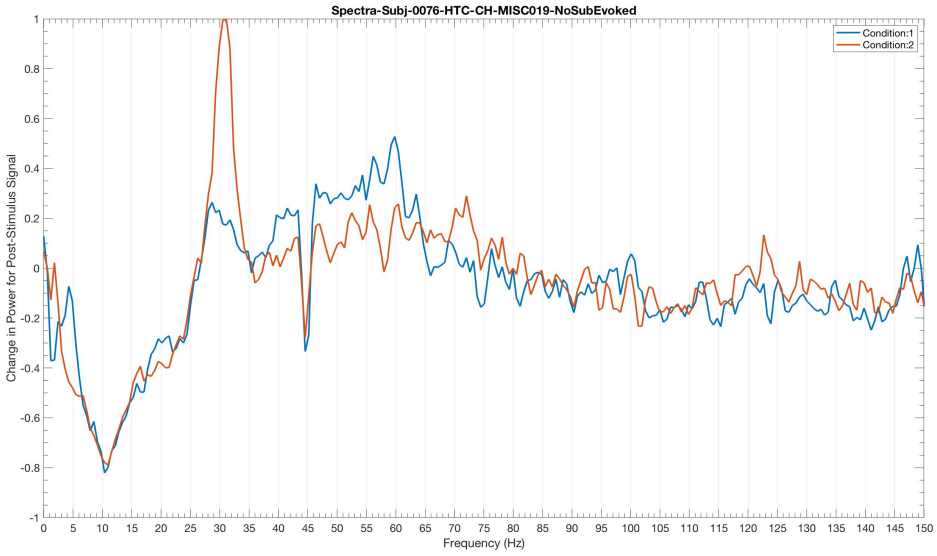

(b)

Figure 8: Power Spectra for NT subject with both conditions: 1 for slow stimulus (blue) and 2 for fast stimulus (red). (a) Low-T_c MEG data (b) High-T_c MEG data. The X-axis reflects frequency (Hz) and Y-axis reflects the average relative post-stimulus change in power. The plots show gamma suppression at around 10 Hz for both low-T_c and high-T_c devices. The gamma activity at around 30 Hz only appears in the high-T_c plot.

The MP data used to generate the plots above was used for further analysis by one of the project supervisors, Dr. Elena Orekhova [38]. The MT method was also previously used to analyze the data and also showed the 30 Hz activity (not shown in this report). However, when analyzed with MP over a short time interval of (0.5 s), the power spectra plot revealed new information as illustrated in figure 9.The plot displays several peaks, some of which are sharp and others with a wider frequency range. This distinction between the different peaks was

less evident when the MT method was previously applied to the data by the research group. The enhanced resolution provided by the MP method allowed to differentiate a wide frequency peak at 30 Hz (low frequency gamma); this would be more likely to be a biological signal rather when compared to noise artifacts, that are usually characterized by sharp peaks. This wide peak seems to be detectable by the high-T_c MEG device only.

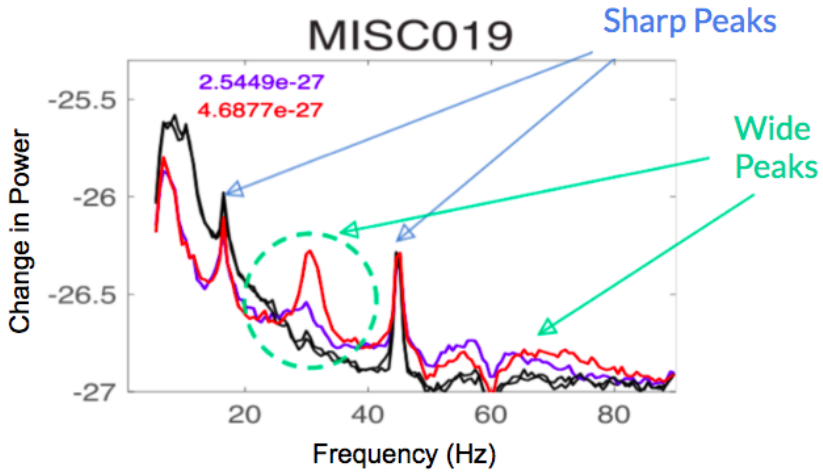

Figure 9: Power Spectra for NT subject at the maximum channel for condition 2 (fast stimulus). The relative change in average post-stimulus power ($log(T^2)$) over frequency is shown for the baseline (black), slow visual stimulation (blue), and fast visual stimulation (red). The plot reveals distinct wide and sharp peaks. Sharp peaks usually indicate noise artifacts while wider peaks are usually associated with biological activity. This leads to the possibility of the 30 Hz peak being more likely a biological signal. However, further analysis is needed to verify this.

3.1.3 Group Comparison of NT and ASD Subjects

The MP algorithm was used for group comparison between NT and ASD subjects. The preliminary results of an ongoing data analysis are reported in this section. The output is shown in figures 10, 11, and 12, which display the group average TF power plots for conditions 1, 2, and 3.

From the plots, one can notice the difference of the frequency range of power increases in the early gamma activity (vertical spikes) between the NT and ASD groups; for all three conditions, the ASD group seems to have the spike concentrated in a lower frequency range than the NT group. Another interesting phenomenon, seen most clearly in figure 10 lies in the late gamma activity (rhythmic component); the frequency seems to be somewhat steady over time for the ASD group while for the NT group, it seems to be decreasing with time. To verify this, Dr. Elena Orekhova [38] performed additional analysis to investigate frequency changes at short time scales (100 ms) in one NT subject (condition 1) and found that the peak frequency of gamma oscillations decreases with time after the beginning of the stimulation as shown in figure 13. Inspecting the figure shows that the peak frequency decreases with time starting from 62 Hz at around 0.2 s after the stimulation begins going down to 57 Hz at around 0.8 s.

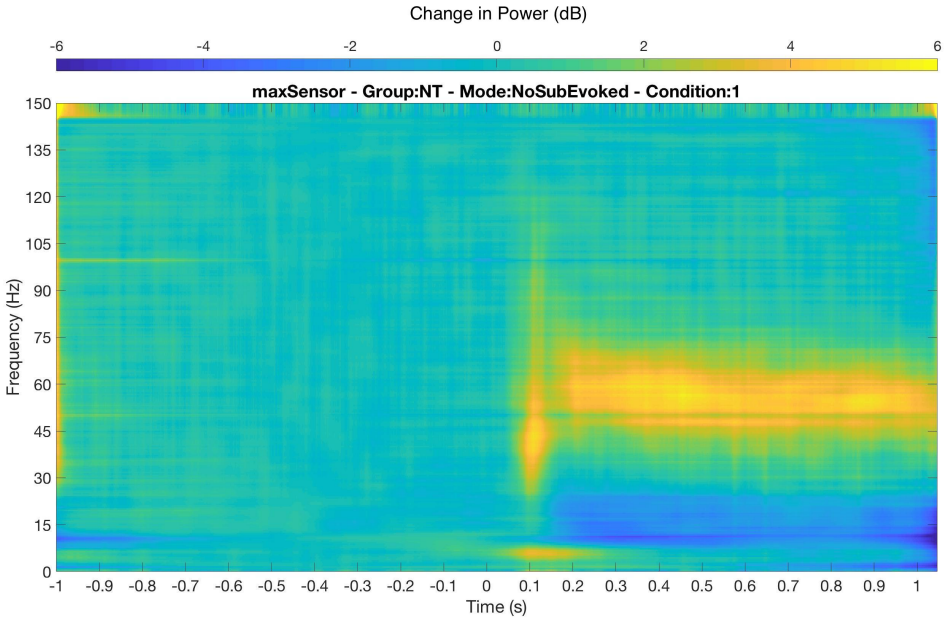

(a)

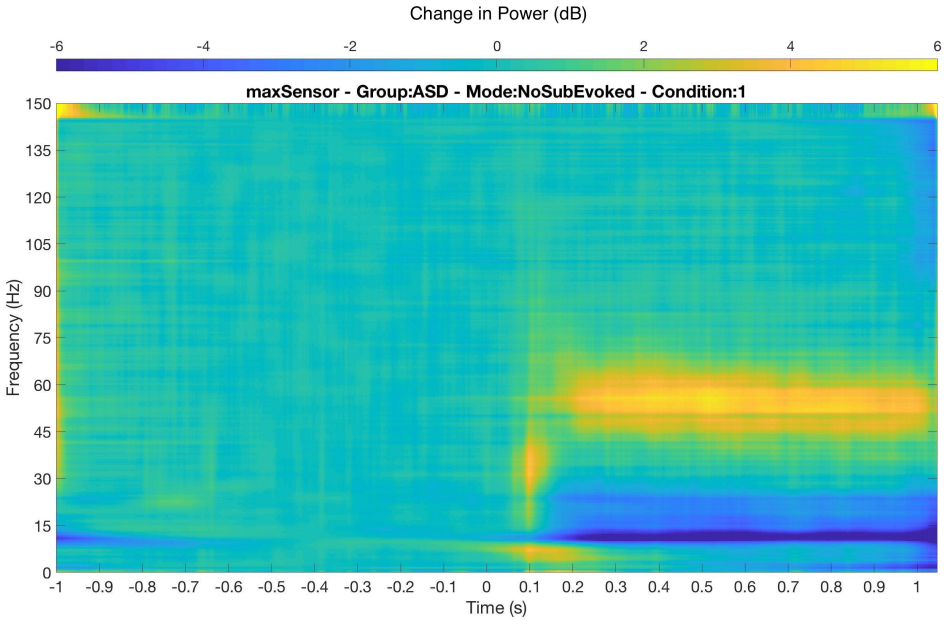

(b)

Figure 10: TF power plots for subject groups taken from the sensor with maximal increase of gamma power (40-90 Hz) for condition 1 (slow stimulus). (a) NT (b) ASD. The color gradient shows the change in power; blue indicates power suppression and yellow indicates increase in power. The plots show that the transient activity in ASD subjects is concentrated at lower frequencies (mainly below 45 Hz) while in NT subjects it extends further to higher frequencies (above 50 Hz). For the late gamma activity, the frequency appears to be steady over time for the ASD group while it decreases with time for the NT group.

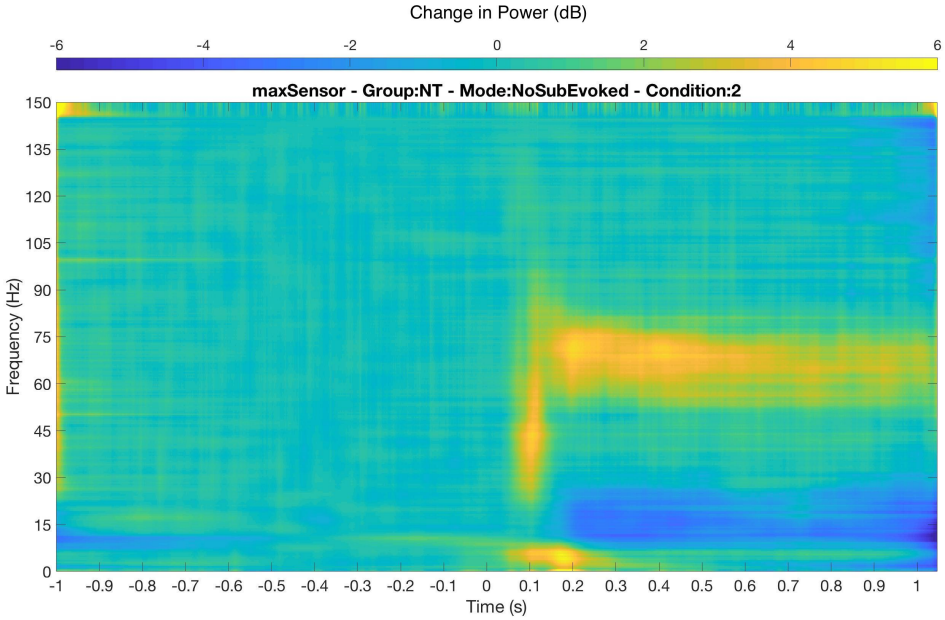

(a)

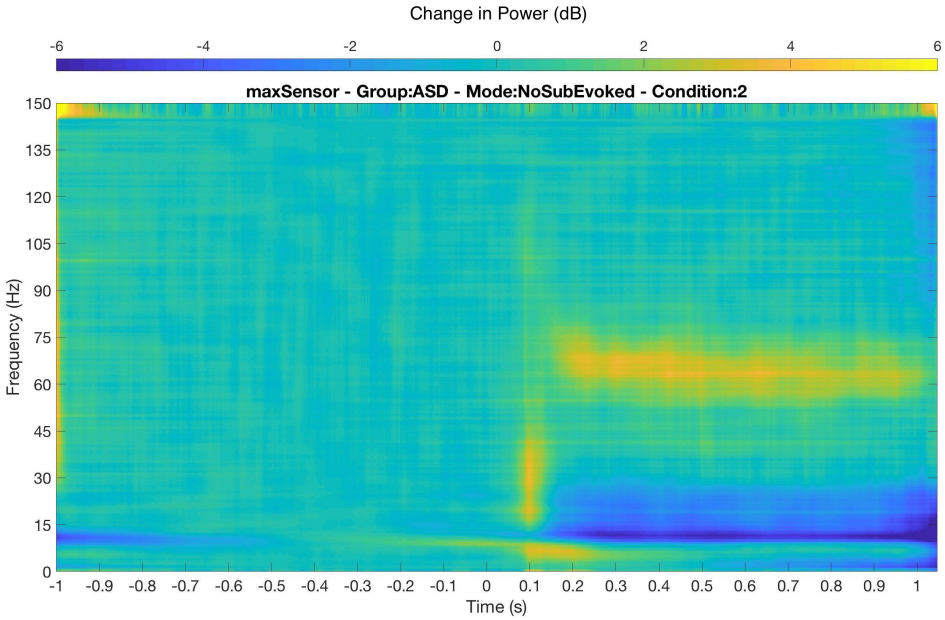

(b)

Figure 11: TF power plots for subject groups taken from the sensor with maximal increase of gamma power (40-90 Hz) for condition 2 (medium speed stimulus). (a) NT (b) ASD. The plots show that the transient activity in ASD subjects is concentrated at lower frequencies (mainly below 45 Hz) while in NT subjects it extends further to higher frequencies (above 50 Hz). For the late gamma activity, the frequency appears to be steady over time for the ASD group while it decreases with time for the NT group. For the late gamma activity, the frequency appears to be steady over time for the ASD group while it decreases with time for the NT group.

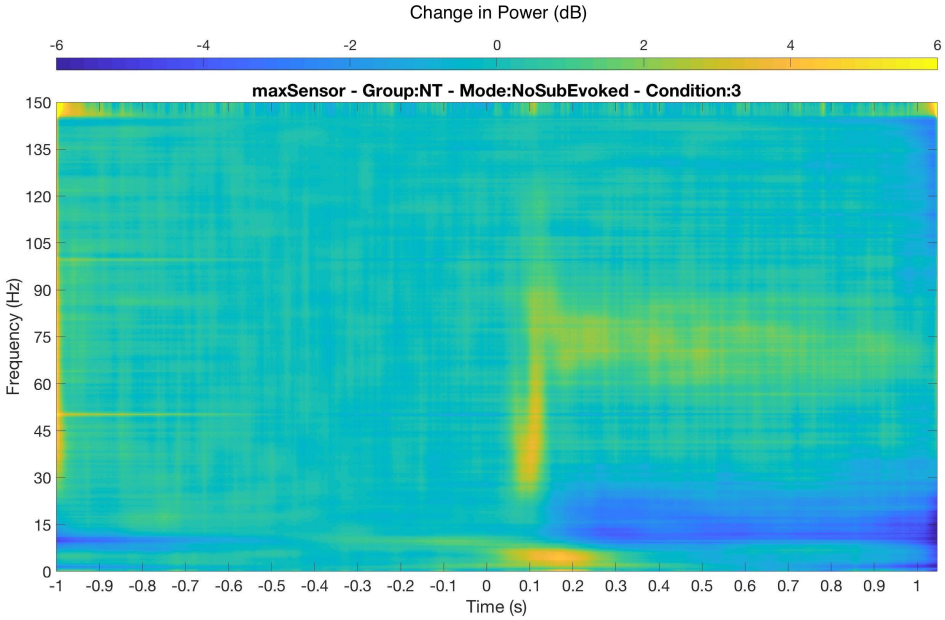

(a)

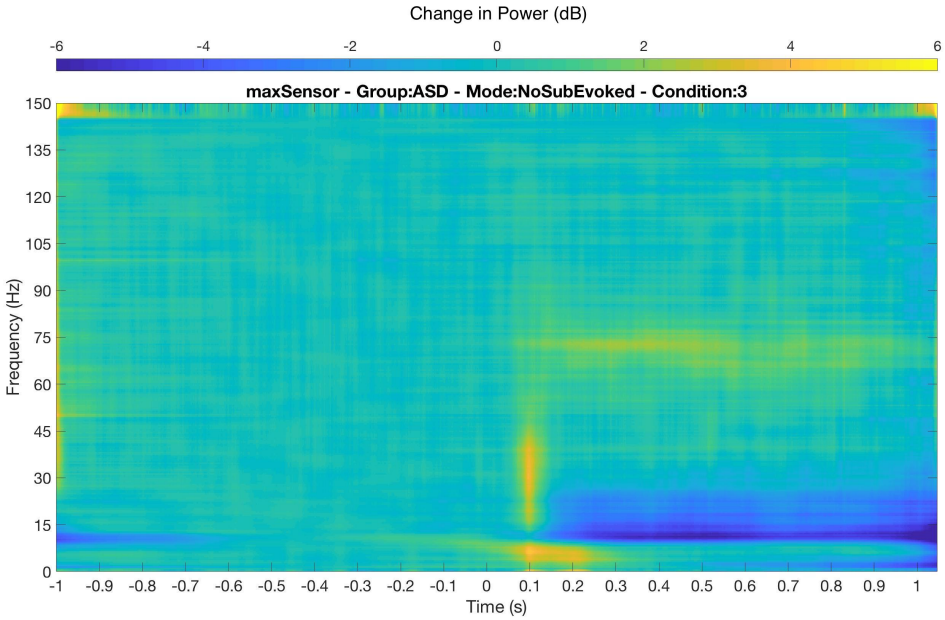

(b)

Figure 12: TF power plots for subject groups taken from the sensor with maximal increase of gamma power (40-90 Hz) for condition 3 (fast stimulus). (a) NT (b) ASD. The plots show that the transient activity in ASD subjects is concentrated at lower frequencies (mainly below 45 Hz) while in NT subjects it extends further to higher frequencies (above 50 Hz). For the late gamma activity, the frequency appears to be steady over time for the ASD group while it decreases with time for the NT group.

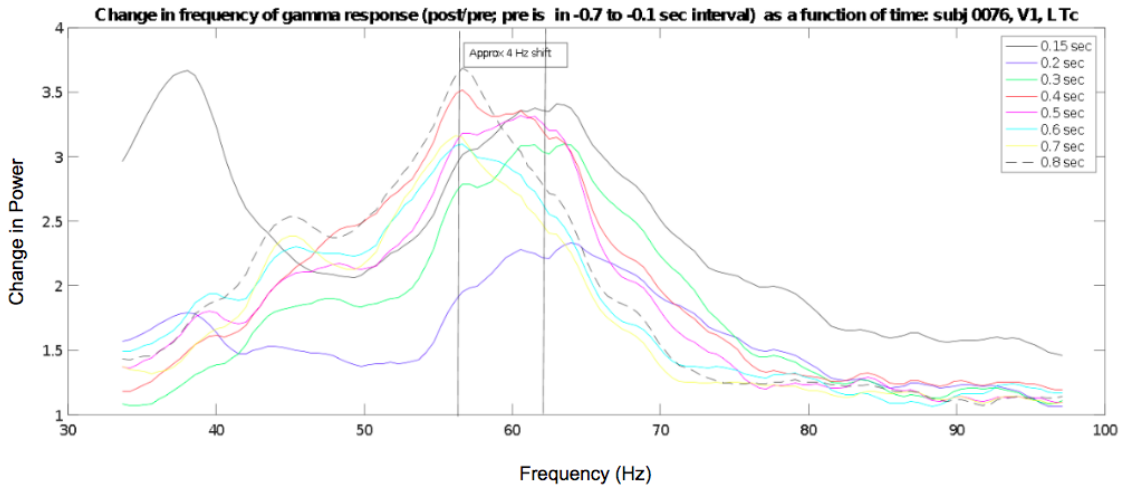

Figure 13: Power spectra for NT subject and condition 1 (slow stimulus). Each line reflects the spectral change in a 100 ms time window after the onset of the stimulus. The legend lists the center times of their corresponding time windows. The vertical lines mark the shift in the induced gamma peak power between early (up to 300 ms) and late (>600 ms) time intervals of the stimulation. This detailed analysis time-based changes only became possible after the application of the MP method. The plot shows that the peak frequency decreases with time starting from 62 Hz at around 0.2 s after the stimulation onset going down to 57 Hz at around 0.8 s.

3.2 Comparison of Dyadic and Stochastic Dictionaries

The results of analyzing MEG data for the same subject and condition using a dyadic and a stochastic dictionary are shown in figures 14, 15, and 16. Figure 14 and 15 display the TF power plots for conditions 1 and 2 respectively, while figure 16 show the power spectra for both conditions.

By inspecting the plots, it can be seen than both methods display more or less similar results for the same number of iterations when it comes to the overall distribution of power change in the TF power plots. However, the power spectra plot shows that the stochastic dictionary curves are smoother than the dyadic dictionary curves for both conditions. Also, the highest peak value is slightly different between the two dictionaries.

From a performance point of view, the results of the dyadic analysis were obtained in around 3 hours, while those of the stochastic analysis required around 4 days of processing. This is similar to the results obtained by Ray, Supratim, et al. 2003 [37], which show that the stochastic implementation is more than 12 times slower than the dyadic one.

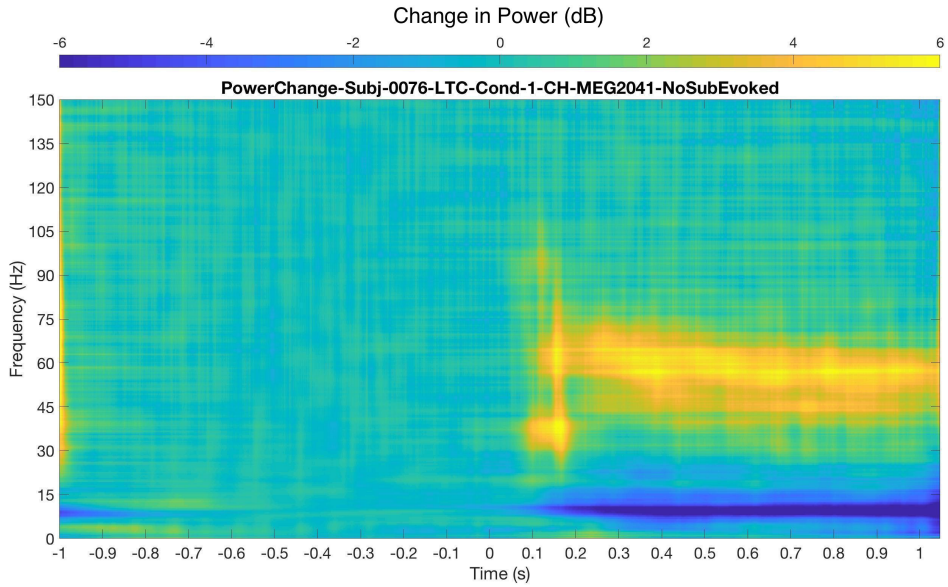

(a)

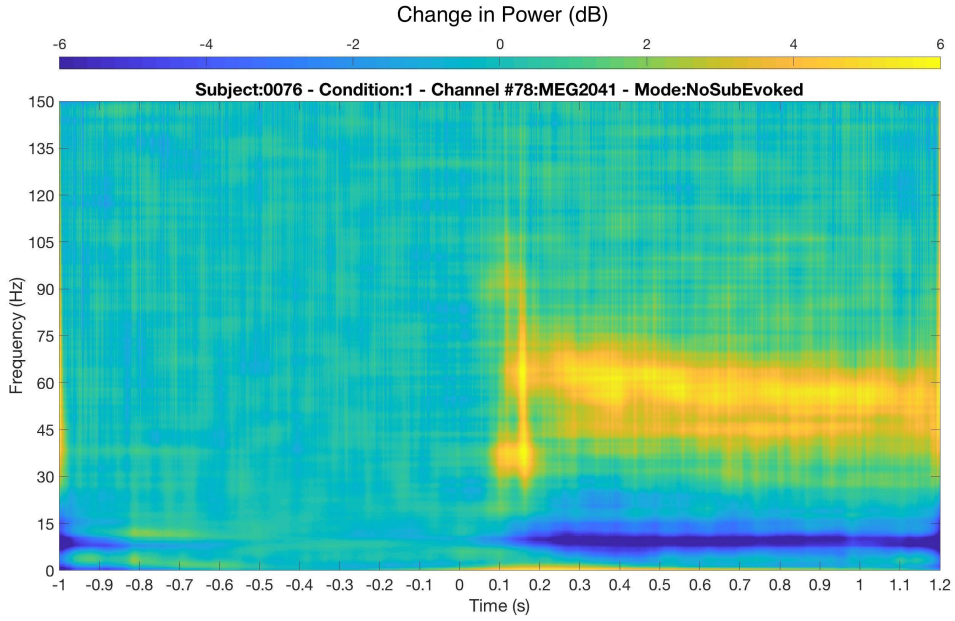

(b)

Figure 14: TF power plots for NT subject and condition 1 (slow stimulus). (a) MP with dyadic dictionary (500 iterations) (b) MP with stochastic dictionary (500 iterations). The color gradient shows the change in power; blue indicates power suppression and yellow indicates increase in power. The plots show that the two methods produce comparable results for the same number of iterations.

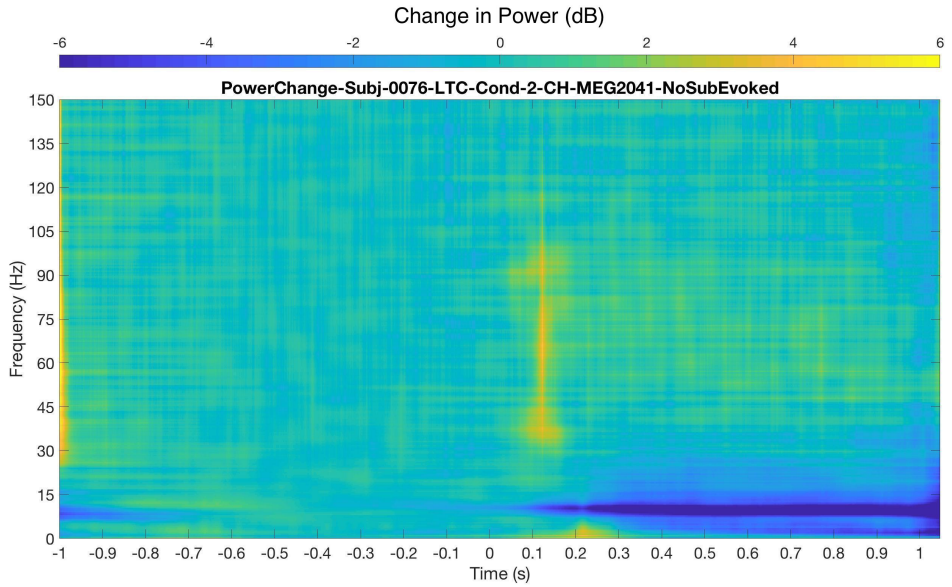

(a)

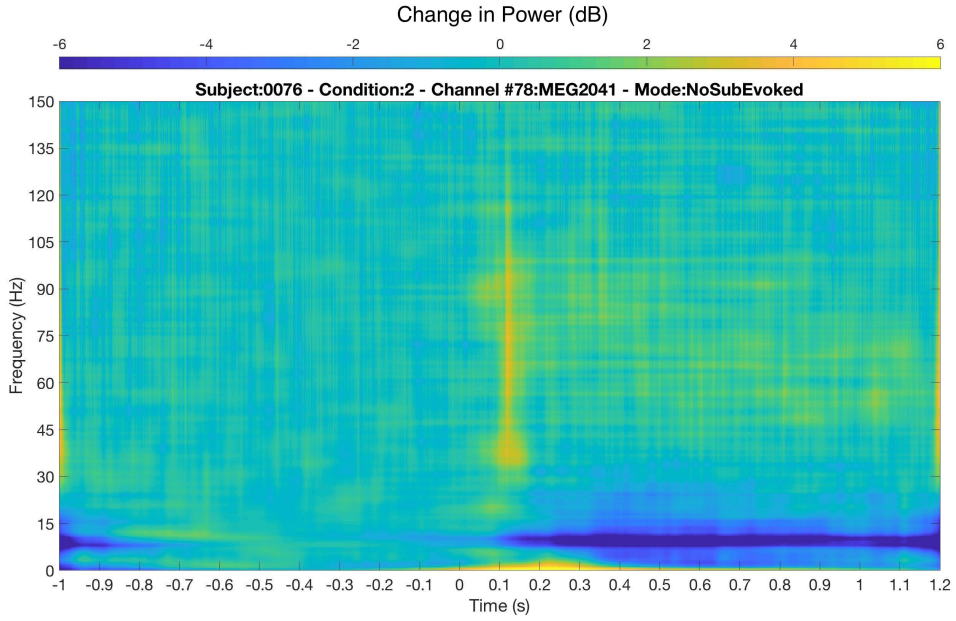

(b)

Figure 15: TF power plots for NT subject and condition 2 (fast stimulus). (a) MP with dyadic dictionary (500 iterations) (b) MP with stochastic dictionary (500 iterations). The plots show that the two methods produce comparable results for the same number of iterations.

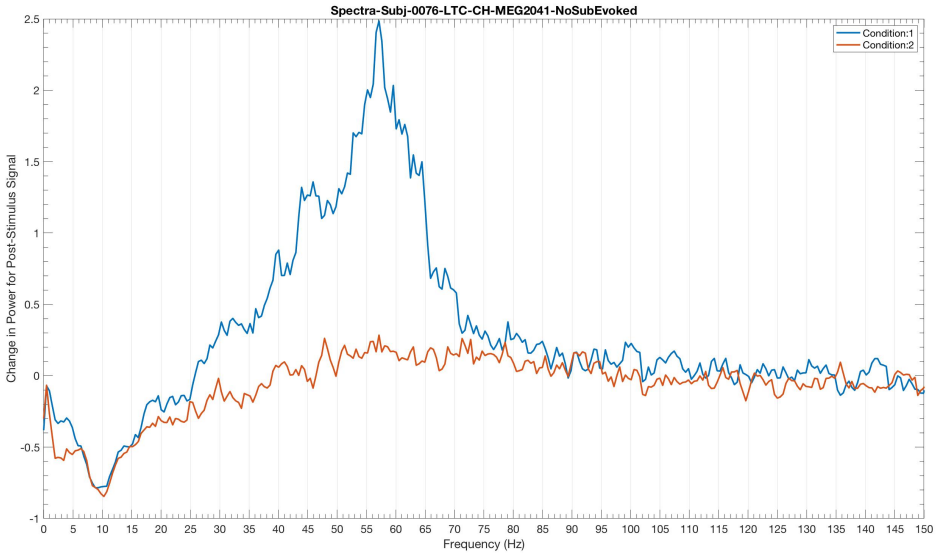

(a)

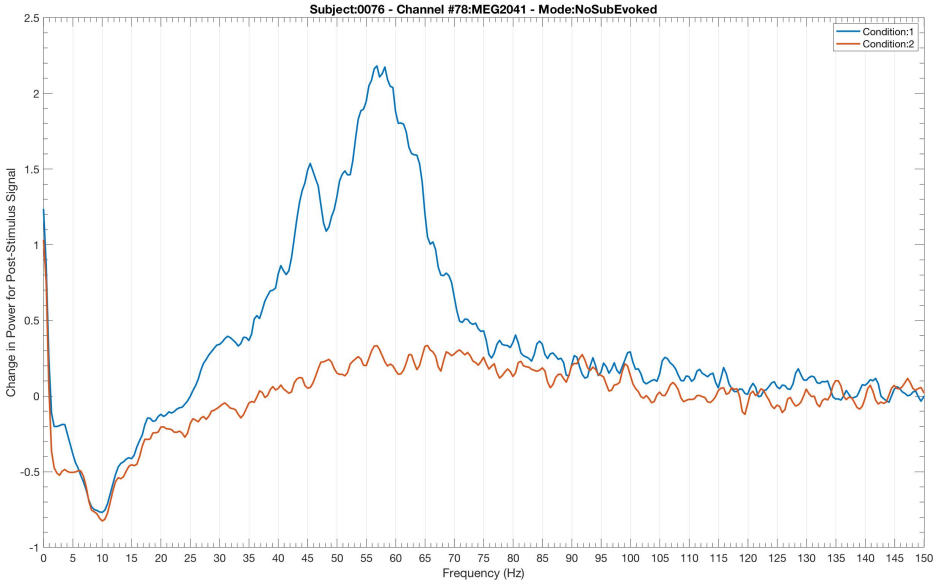

(b)

Figure 16: Power Spectra for NT subject and 2 conditions: 1 for slow stimulus (blue) and 2 for fast stimulus (red). (a) MP with dyadic dictionary (500 iterations) (b) MP with stochastic dictionary (500 iterations). The X-axis reflects frequency (Hz) and Y-axis reflects the average relative post-stimulus change in power. The plots show that the two methods produce comparable results for the same number of iterations.

In line with the results above, it has been found that both dictionaries produce comparable results. However, the long execution time of the stochastic dictionary makes the application of the dyadic dictionary more practical in general and sufficient for the analysis tasks at hand.

4 Discussion

MEG provides a noninvasive brain-imaging technique for monitoring and studying brain activity. To achieve that, TF analysis is performed to extract informative spatiotemporal spectral patterns that may be useful for neuroscience or clinical investigations. The complex nature of the recorded signals - due to subject variability, nonstationarity of the signal, and high dimensionality of data - poses substantial challenges for researchers and thus requires improvement of current analysis techniques and innovation of more suitable analysis tools.

In this project, the MP algorithm is used as an attempt to overcome the time-frequency resolution limitations faced when using standard TF analysis techniques. As shown by Chandran et al., 2016, the method was successful in providing better time and frequency resolutions when applied to EEG data recorded from monkeys. By adapting and applying the software described by Chandran et al., 2016 [5] and Chandran Ks et al., 2017 [20] to MEG data recorded from human subjects and comparing it to the MT method, similar improvements in both resolutions were observed and the analysis was able to capture rhythmic and transient components at the same time as expected. The output was also consistent with the MT output in terms of overall power change in response to stimuli. Unlike standard methods - such as the FT, STFT, MT, and WT techniques - improving the resolution of one dimension (time or frequency) does not result in any perceivable degradation in the other. The key factor for improving both time and frequency resolutions is the use of an adaptive method that covers the time–frequency space of the signal as much as possible; MP and its accompanying dictionary of atoms provides this flexibility to adapt to local time and frequency properties of the signal.

The potential usefulness of the MP method has been demonstrated for two applications: the detection of brain signals in MEG recordings using the high-T_c technology currently under development and the comparison between clinical (ASD) and control groups (NT) of subjects.

When MP was used for the low-T_c and high-T_c MEG data comparison, the method was able to provide higher frequency resolution that allowed the subsequent analysis performed by Elena Orekhova [38] to reveal distinct sharp and wide peaks in the power spectra of the signals, which were less evident when using the MT method. This might indicate that the activity captured by the high-T_c device around 30 Hz as shown in figures 7 and 8 could be a true signal reflecting biological activity as it has a relatively wide peak (see figure 9) when compared to artifacts, which are usually characterized by their sharp peaks. These findings require further investigation before any solid conclusions can be made but they provide a starting point to explore whether or not high-T_c MEG sensors may detect additional signals as a result of their closer and more localized positioning with respect to the scalp compared to low-T_c sensors. Additionally, the results show that the sharp peaks (high-amplitude artifacts) may result in a distorted gamma

response spectrum, which adds to the complexity of making reliable estimations of power changes and corresponding frequency values. From another perspective, the high-T_c device does not capture the early gamma transient component that is seen in the low-T_c plots despite MP's sensitivity to transient components and its detection of power suppression in data from both devices. The reason could be that the high-T_c sensor under development provides a lower signal to noise ratio and perhaps the sensor localization on the scalp was not optimal to capture all components of the signal. Finally, the data available for testing high-T_c MEG data was very limited; recordings from three subjects only were available with two of them having high noise interference. Therefore, this analysis should be repeated and additional studies should be done once more data of higher quality is available.

For the following experiment, the application of MP for the group comparison between NT and ASD subjects allowed enhanced inspection of the early transient component of the gamma rhythm due to the improved time and frequency resolutions the method provides. This revealed a possible feature that may help in distinguishing between the two groups based on differences in early gamma activity; this is seen in the location differences of the vertical spikes with respect to the frequency axis as shown in figures 10, 11, and 12. MP also allowed tracking frequency changes in the gamma response over 100 ms time windows. The perceived drop in frequency values over time in the late gamma activity (rhythmic component) of the NT group may be related to inhibitory processes. Ongoing analysis within the research group will reveal whether the temporal courses of gamma frequency and power are consistently different between the ASD and NT groups. If so, this may reflect differences in the regulation of the E-I balance between the two groups. As the early and late gamma responses convey different information, both components can be useful to describe putative changes in brain function in ASD subjects. As with the previous experiment, the findings require further investigation before any concrete conclusions can be made.

The final experiment shows that the output of the dyadic dictionary produces is very comparable to the stochastic dictionary's output. The differences in the outputs can be mainly attributed to the difference in the size of dictionaries and the sampling technique used for each dictionary. Due to the greater size of its dictionary, its uniform sampling strategy, and the process of atom parameter randomization, the MP implementation that uses the stochastic dictionary is able to produce more suitable and less biased reconstructions of the signals being analyzed than the dyadic dictionary. However, this all comes at a the cost of execution time. Therefore, it might be sufficient to use a dyadic dictionary for an overall inspection of the signal and the stochastic dictionary can be used when certain features need to be inspected more closely in smaller segments of the signal. However, if the dyadic dictionary is used one must take into consideration the sampling frequency and the inter-stimulus interval length that would produce a signal that has at least the minimum length that accommodates the power of 2 condition without losing essential parts of the data. For the stochastic dictio-

nary, since its size is usually significantly large, it would be worth investigating quantifiable measures to specify the minimum size that would result in the minimum bias while maintaining high accuracy and reasonable execution time.

Despite MP's ability to provide improved results, there are some limitations in the current implementation that need to be considered. First, the choice of dictionary affects the quality of the output and therefore it should be designed to suit nature of the signal being studied. For the current implementation, it could be worthwhile to explore other dictionaries that could add to the accuracy of the signal reconstruction. Second, the dictionaries used in this project are predefined i.e. based on Gabor functions. Including adaptive dictionaries based on different functions may be another option to obtain more suitable atom matches that would lead to better signal estimation. Third, to address the phase coupling issue, it may be necessary to use other TF analysis method or explore how MP may be adjusted to handle this case when needed. Fourth, for MP to be useful for clinical use and research, its performance should be optimized to run the analysis in a shorter time without compromising the quality of the output. Although the performance of the different techniques has not been explicitly compared in this project as the main goal was to verify the improved quality of the TF analysis, it can still be seen that the MP method is computationally intensive and time consuming especially when higher accuracy is needed. Also, memory usage should be taken into consideration as MEG datasets tend to be large in size; one trial usually involves a 2D TF matrix with dimensions in the order of O(several thousands x several hundreds) for recordings that are only a few seconds in length and experiments usually include hundreds of trials for multiple conditions per subject.

With regards to the current project work, the full code of this project is publicly available and may be downloaded as indicated in the methods section. Information regarding the use of key parameters is covered in the methods section of the report. Additional usage support is provided in the form of comments in the source code. However, following are some key points to keep in mind when using the software (relevant details are available in the code comments). First, dataset formats should be compatible with or manipulated to match the format used in the software. It is recommended to use datasets that have the same number of points and obtained using the same sampling frequency when data comparisons are performed. The number of MP iterations may be reduced by the user for reduced execution time, however, if this number is too low, then the signal approximation may not provide an accurate representation of the signal analyzed. Additionally, reducing the dictionary size may also result in shorter execution times but caution should be taken to ensure that that bias is minimized. The size is dependent on the signal length for the dyadic dictionary and on the specified parameter dictionarySize for the stochastic dictionary. Finally, the software includes options to save intermediate and final output data in addition to figures in folders with user-specified names to allow output reuse and to avoid file overwrites when needed.

Possible future work should explore other available implementations and variations of the MP algorithm that may have been optimized for enhanced performance, flexibility, and quality. This project relied on basic implementations of the MP algorithm as a proof of concept based on its documented success in EEG signal analysis. Other possibilities would include the exploration of other aspects of gamma oscillations (e.g. durations) and other types of oscillations using the MP method to explore whether it can reveal new features that may not have been capture using the standard methods described in this project. From a usability point of view, the code should be packaged in a user-friendly manner for general use by the scientific community and also to reduce the possibility of manual errors when adjusting analysis parameters. Once the method is well-established, this could offer new opportunities for machine learning and big-data in the field of MEG imaging e.g. for the automation of diagnosis and large scale studies. It would also open the door for the use of MEG to study a wider range of brain diseases. This, however, relies heavily on interdisciplinary collaboration to provide reliable interpretations of the signals analyzed.

5 Conclusion

MP offers potential insights that are not easily captured using some of the currently-used standard techniques. This is a positive step towards providing more reliable tools that are capable of characterizing neurological disorders and improving the diagnosis and treatment of brain disorders. This also opens the door for further explorations of signal components that may have not been detectable with other methods. All in all, MP provides several advantages and more efforts are needed to optimize this method and to establish other methods that can enhance the reliability and usability of MEG data. Also, new sensor technologies that bring MEG devices closer to the scalp have the potential to provide signals of better strength and perhaps detect signals that are not attainable otherwise. The results obtained so far are encouraging, thus, more efforts are needed to enhance both hardware and software components to leverage the benefits of MEG imaging.

References

[1] Monica Di Luca, David Nutt, Wolfgang Oertel, Patrice Boyer, Joke Jaarsma, Frederic Destrebecq, Giovanni Esposito, and Vinciane Quoidbach. Towards earlier diagnosis and treatment of disorders of the brain. *Bulletin of the World Health Organization*, 96(5):298, 2018.

[2] Monica DiLuca and Jes Olesen. The cost of brain diseases: a burden or a challenge? *Neuron*, 82(6):1205–1208, 2014.

[3] Sylvain Baillet. Magnetoencephalography for brain electrophysiology and imaging. *Nature neuroscience*, 20(3):327, 2017.

[4] Boualem Boashash. *Time-frequency signal analysis and processing: a comprehensive reference*. Academic Press, 2015.

[5] Subhash Chandran KS, Ashutosh Mishra, Vinay Shirhatti, and Supratim Ray. Comparison of matching pursuit algorithm with other signal processing techniques for computation of the time-frequency power spectrum of brain signals. *Journal of Neuroscience*, 36(12):3399–3408, 2016.

[6] Christoph Pfeiffer, Silvia Ruffieux, Lars Jönsson, Maxim L Chukharkin, Alexei Kalaboukhov, Minshu Xie, Dag Winkler, and Justin F Schneiderman. A 7-channel high-tc squid-based on-scalp meg system. *bioRxiv*, page 534107, 2019.

[7] G.J. Tortora and B.H. Derrickson. *Introduction to the Human Body, 8th Edition*. Wiley, 2010.

[8] Gyorgy Buzsaki. *Rhythms of the Brain*. Oxford University Press, 2006.

[9] Wikipedia. Neural oscillation. `https://en.wikipedia.org/wiki/Neural_oscillation`.

[10] Fernando Lopes da Silva. Eeg and meg: relevance to neuroscience. *Neuron*, 80(5):1112–1128, 2013.

[11] S Karakaş, C Başar-Eroğlu, C Özesmi, H Kafadar, and Ö Ü Erzengin. Gamma response of the brain: a multifunctional oscillation that represents bottom-up with top-down processing. *International Journal of Psychophysiology*, 39(2-3):137–150, 2001.

[12] Elena V Orekhova, Tatiana A Stroganova, Justin F Schneiderman, Sebastian Lundström, Bushra Riaz, Darko Sarovic, Olga V Sysoeva, Georg Brant, Christopher Gillberg, and Nouchine Hadjikhani. Neural gain control measured through cortical gamma oscillations is associated with sensory sensitivity. *Human brain mapping*, 40(5):1583–1593, 2019.

[13] Wikipedia. Fourier transform. `https://en.wikipedia.org/wiki/Fourier_transform`.

[14] Wikipedia. Dot product. https://en.wikipedia.org/wiki/Dot_product.

[15] Wikipedia. Parseval's theorem. https://en.wikipedia.org/wiki/Parseval%27s_theorem.

[16] Marieke K van Vugt, Per B Sederberg, and Michael J Kahana. Comparison of spectral analysis methods for characterizing brain oscillations. *Journal of neuroscience methods*, 162(1-2):49–63, 2007.

[17] Fieldtrip. Time-frequency analysis using hanning window, multitapers and wavelets. http://www.fieldtriptoolbox.org/tutorial/timefrequencyanalysis/.

[18] Stéphane G Mallat and Zhifeng Zhang. Matching pursuits with time-frequency dictionaries. *IEEE Transactions on signal processing*, 41(12):3397–3415, 1993.

[19] Wikipedia. Hilbert space. https://en.wikipedia.org/wiki/Hilbert_space.

[20] Subhash Chandran KS, Chandra Sekhar Seelamantula, and Supratim Ray. Duration analysis using matching pursuit algorithm reveals longer bouts of gamma rhythm. *Journal of neurophysiology*, 119(3):808–821, 2017.

[21] Piotr J Durka, Dobieslaw Ircha, and Katarzyna J Blinowska. Stochastic time-frequency dictionaries for matching pursuit. *IEEE Transactions on Signal Processing*, 49(3):507–510, 2001.

[22] Gagan Rath and Arabinda Sahoo. A comparative study of some greedy pursuit algorithms for sparse approximation. In *2009 17th European Signal Processing Conference*, pages 398–402. IEEE, 2009.

[23] Leon Cohen. Time-frequency distributions-a review. *Proceedings of the IEEE*, 77(7):941–981, 1989.

[24] Wolfgang Martin and Patrick Flandrin. Wigner-ville spectral analysis of nonstationary processes. *IEEE Transactions on Acoustics, Speech, and Signal Processing*, 33(6):1461–1470, 1985.

[25] Wikipedia. Discrete fourier transform. https://en.wikipedia.org/wiki/Discrete_Fourier_transform.

[26] Siddhesh Salelkar, Gowri Manohari Somasekhar, and Supratim Ray. Distinct frequency bands in the local field potential are differently tuned to stimulus drift rate. *Journal of neurophysiology*, 120(2):681–692, 2018.

[27] Google. Google web search. https://www.google.com/.

[28] Google. Google scholar. https://scholar.google.se/.

[29] Chalmers University of Technology. Online library - chalmers university of technology. http://www.lib.chalmers.se/.

[30] Mathworks. Matlab. https://www.mathworks.com/products/matlab.html.

[31] Subhash Chandran KS, Ashutosh Mishra, Vinay Shirhatti, and Supratim Ray. Matching pursuit software with a dyadic dictionary implementation. https://github.com/supratimray/MP.

[32] Subhash Chandran KS, Chandra Sekhar Seelamantula, and Supratim Ray. Matching pursuit software with a stochastic dictionary implementation. https://github.com/supratimray/GammaLengthProjectCodes.

[33] Elena V Orekhova, Olga V Sysoeva, Justin F Schneiderman, Sebastian Lundström, Ilia A Galuta, Dzerasa E Goiaeva, Andrey O Prokofyev, Bushra Riaz, Courtney Keeler, Nouchine Hadjikhani, et al. Input-dependent modulation of meg gamma oscillations reflects gain control in the visual cortex. *Scientific reports*, 8(1):8451, 2018.

[34] Fieldtrip. Time-frequency analysis iii using multitapers. http://www.fieldtriptoolbox.org/tutorial/timefrequencyanalysis/#multitapers.

[35] Robert Oostenveld, Pascal Fries, Eric Maris, and Jan-Mathijs Schoffelen. Fieldtrip: open source software for advanced analysis of meg, eeg, and invasive electrophysiological data. *Computational intelligence and neuroscience*, 2011:1, 2011.

[36] Fieldtrip. Fieldtrip documentation. http://www.fieldtriptoolbox.org/reference/.

[37] Supratim Ray, Christophe C Jouny, Nathan E Crone, Dana Boatman, Nitish V Thakor, and Piotr J Franaszczuk. Human ecog analysis during speech perception using matching pursuit: a comparison between stochastic and dyadic dictionaries. *IEEE transactions on biomedical engineering*, 50(12):1371–1373, 2003.

[38] Gillberg Neuropsychiatry Centre. Elena orekhova. https://gillbergcentre.gu.se/english/research-staff-%26-associates/orekhova--elena.

[39] Wikipedia. Newton's method in optimization. https://en.wikipedia.org/wiki/Newton%27s_method_in_optimization.

A Appendix

In this appendix, some of the theory behind the methods used in the project are clarified in some more details.

A.1 General Concepts

This part clarifies some general mathematical and frequency domain concepts.

A.1.1 Inner Product of Complex Functions

The inner (or dot) product [14] of vectors is defined as the sum of the products of corresponding vector components. For continuous functions it is defined as the integral of the product over a given interval. This concept can be extended to complex functions (f and g) to obtain the inner product as:

$$< f, g >= \int_{-\infty}^{+\infty} f(t)\bar{g}(t)dt \tag{5}$$

where $\bar{g}(t)$ is the complex conjugate of the function g(t). This is similar for the case of discrete functions:

$$< f, g >= \sum_{n=0}^{N-1} f[n]\bar{g}[n] \tag{6}$$

where $\bar{g}[n]$ is the complex conjugate of g[n] and both f and g are of the length N.

A.1.2 Parseval's Theorem

Parseval's Theorem [15] sates that the integral (or sum) of the square value of a function f(t) equals the integral (or sum) of the square value of its Fourier transform F(w). Thus, the total energy of a signal f(t) is conserved after a FT is performed and may be defined for continuous functions as:

$$E = \int_{-\infty}^{+\infty} |f(t)|^2 dt = \int_{-\infty}^{+\infty} |F(\omega)|^2 d\omega \tag{7}$$

Here, $|f(t)|^2$ represents the instantaneous power, which reflects how the energy of the signal is distributed over time. $|F(\omega)|^2$ is the power spectral density (PSD), which shows the power concentrated at different frequencies in the signal. The same concept applies to discrete signals:

$$E = \sum_{n=0}^{N-1} |x[n]|^2 = \frac{1}{N} \sum_{k=0}^{N-1} |X[k]|^2 \tag{8}$$

where X[k] is the DFT of x[n], both of length N.

A.1.3 Hilbert Space

A Hilbert space [18][19] is an abstract vector space that extends two-dimensional and three-dimensional spaces and their associated methods and techniques to spaces having any finite or infinite number of dimensions. It has the structure of an inner product that permits the measurement of length and angle; this follows from the inner product being the sum of the products of corresponding elements of two sequences of numbers from an algebraic point of view but also from it being the product of the magnitudes of two vectors and the cosine of the angle between them from a geometrical point of view. Points in the space are infinite sequences of real numbers that are square summable, such that for an infinite series, the sum of the squares converges to a finite number.

Each Hilbert space has an orthonormal basis, which is a family of elements in the space that satisfy normalization to 1, pair-wise orthoganility, and completeness (partial sums converge to an element of the space). Every vector in the Hilbert space can be expressed uniquely as an infinite linear combination of the vectors in the basis or in other words as the sum of multiples of the basis vectors.

For function spaces, $L^2(R)$ is the Hilbert space of complex valued functions where:

$$||f|| = \int_{-\infty}^{+\infty} |f(t)|^2 dt < +\infty \tag{9}$$

A.2 Signal Decomposition and Reconstruction

Here, the theory behind Matching Pursuit (MP) signal decomposition and energy reconstruction are described [5][18][20][21].

A.2.1 Matching Pursuit for Signal Decomposition

Below is a simplified summary of the theory behind the Matching Pursuit Algorithm used for signal decomposition. Let:

- H be a Hilbert space such that H = $L^2(R)$ (see Appendix A.1.3).
- f be the function or signal to be decomposed such that $f \in H$ and f is of the length N i.e. N = number of samples in the signal. N also reflects the number of dimensions in H.
- g be a window function that is continuously differentiable with $||g|| = 1$ (normalized to unity). Also, the integral of g is nonzero and g(0) is nonzero.
- D be a dictionary of time-frequency atoms where $D = (g_\gamma)_{\gamma \in \Gamma}$.
- γ be and index such that $\gamma = (s, u, \xi)$, where s is for scaling, u is for translation, and ξ is for frequency modulation.

- $\Gamma = R^+ \times R^2$, where R^+ refers to the positive real numbers and R^2 refers to the two-dimensional real space.

The goal is to compute a linear expansion of f over a set of atoms from D that match its inner structures in the best possible way using successive approximations of f. To clarify this concept, let us start with one atom $g_{\gamma_0} \in D$. f Can be decomposed as follows:

$$f =< f, g_{\gamma_0} > g_{\gamma_0} + Rf \tag{10}$$

$< f, g_{\gamma_0} >$, the inner product, represents how f and g_{γ_0} correlate or in other words how much of f is explained by g_{γ_0}. Thus, the term $< f, g_{\gamma_0} > g_{\gamma_0}$ represents the part of the function f that has been explained by g_{γ_0}. Finally, Rf is the remaining residue after approximating f using g_{γ_0} i.e. after the part explained by g_{γ_0} has been removed from the function f.

It is important to note that g_{γ_0} is orthogonal to Rf. Therefore,

$$||f||^2 = | < f, g_{\gamma_0} > |^2 + ||Rf||^2 \tag{11}$$

In order minimize $||Rf||$, g_{γ_0} should be selected from D such that $| < f, g_{\gamma_0} > |$ is maximized. Sometimes, it is only possible the closest best match:

$$| < f, g_{\gamma_0} > | \geq \alpha sup_{\gamma \in \Gamma} | < f, g_\gamma > | \tag{12}$$

Where α is an optimality factor such that $0 < \alpha \leq 1$ and the supremum (sup) refers to the least upper bound. g_{γ_0} is selected based on a choice function that differs depending on the numerical implementation.

This process is repeated every time an atom is matched and a new residue is obtained. For the n^{th} order residue ($n \geq 0$), the choice function selects an element $\gamma_n \in D$ that closely matches that residue:

$$| < R^n f, g_{\gamma_n} > | \geq \alpha sup_{\gamma \in \Gamma} | < R^n f, g_\gamma > | \tag{13}$$

At the end, MP decomposes the function f into a sum of complex time-frequency atoms that best match its residues as:

$$f = \sum_{n=0}^{+\infty} < R^n f, g_{\gamma_n} > g_{\gamma_n} \tag{14}$$

where $\gamma_n = (s_n, u_n, \xi_n)$, expansion coefficients are reflected by $< R^n f, g_{\gamma_n} >$, and

$$g_{\gamma_n}(t) = \frac{1}{\sqrt{s_n}} g(\frac{t - u_n}{s_n}) e^{i\xi_n t} \tag{15}$$

with $\frac{1}{\sqrt{s_n}}$ being the normalization factor and t referring to time.

To further understand this technique, one must investigate what happens over

the iterations. At n = 0, $< f, g_{\gamma_0} > g_{\gamma_0}$ is set to 0 and therefore $R^0 f$ = f. Next $R^0 f$ is decomposed using an atom to produce the following residue $R^1 f$ and so on. At any iteration, the decomposition of a residue generalizes to:

$$R^n f =< R^n f, g_{\gamma_n} > g_{\gamma_n} + R^{n+1} f \tag{16}$$

where g_{γ_n} is orthogonal to $R^{n+1} f$, the following residue. Thus,

$$||R^n f||^2 = | < R^n f, g_{\gamma_n} > |^2 + ||R^{n+1} f||^2 \tag{17}$$

As n increases, the residue decays exponentially.

If this operation is carried out to an order of $n = m$, from equation the approximation of function f may be expressed as:

$$f = \sum_{n=0}^{m-1} < R^n f, g_{\gamma_n} > g_{\gamma_n} + R^m f \tag{18}$$

Again, $||f||^2$ can be written as a concatenated sum yielding energy conservation:

$$||f||^2 = \sum_{n=0}^{m-1} | < R^n f, g_{\gamma_n} > |^2 + ||R^m f||^2 \tag{19}$$

When a dictionary is very redundant, the search for the best match can be limited to a subset $D_\alpha \subset D$. Depending on the optimality factor and the dictionary redundancy, the set of best matching atoms D_α can be much smaller than D. This is done by initializing the Matching Pursuit algorithm with the inner products of f with $g_\gamma \in D_\alpha$. D_α is searched for an atom $g_{\bar{\gamma}_n}$ that best matches the current residue; i.e. it identifies the approximate scale, time, and frequency localization of the main structures of f. To further improve the match, Newton's method in optimization [39] is used to identify and index γ_n in the vicinity of $\bar{\gamma}_n$ that results in a local maximum for $| < f, g_\gamma > |$. The choice function mentioned above is implicitly defined by this double-search scheme.

Once $g_{\gamma_n} \in D$ is selected, the inner product of the new (following) residue with any $g_\gamma \in D_\alpha$ and the inner product is updated based on equation 16 to yield:

$$< R^{n+1} f, g_\gamma >=< R^n f, g_\gamma > - < R^n f, g_{\gamma_n} >< g_{\gamma_n}, g_\gamma > \tag{20}$$

where the only value left to calculate is $< g_{\gamma_n}, g_\gamma >$as other values have already been computed previously. Dictionaries are usually design to ensure that this inner product is obtained using a small number of operations. The number of times a residue is sub-decomposed depends on the desired precision and the number of iterations also depends on the decay rate of $||R^n f||$, which in turn depends on the correlation between the residues and the atoms in the dictionary and is measured by the correlation ratio $\lambda(f)$:

$$\lambda(R^n f) = sup_{\gamma \in \Gamma} \frac{| < R^n f, g_\gamma > |}{||R^n f||} \tag{21}$$

The lower the correlation ratios of a given signal f and its residues, the slower the decay, which would require further expansion for better approximation of the signal; i.e. the information in f is diluted over the dictionary. However, the number of iterations is usually much less than N is most cases.

A.2.2 Wigner-Ville Distribution for Signal Reconstruction

The energy reconstruction of decomposed signals is computed using the Wigner-Ville distribution (WVD) in both dyadic and stochastic implementations. Here, the pseudo WVD used in the works of Chandran et al., 2016 [5][31] is described to clarify the general concept behind its application in the reconstruction process.

The window function used is a Gaussian window as defined below:

$$g(t) = 2^{\frac{1}{4}} e^{-\pi t^2} \tag{22}$$

where t is the time.

Define a function Wg(t,w) as:

$$Wg(t, \omega) = 2e^{-2\pi(t^2 + (\frac{\omega}{2\pi})^2)} \tag{23}$$

where t is the time and ω the frequency.

The atoms used for the dyadic implementation of MP are real atoms - cosine modulated functions - and are defined as follows:

$$g_{\gamma,\phi} = g(\frac{t-u}{s}) cos(\xi t + \phi) \tag{24}$$

Here, t is the time, ϕ is the phase, and γ is an index such that $\gamma = (s, u, \xi)$. The indices represented by γ are: s for scaling, u for translation, and ξ for frequency modulation.

A Matching Pursuit implementation using this dictionary would decompose a signal f(t) to:

$$f = \sum_{n=0}^{+\infty} < R^n f, g_{(\gamma_n, \phi_n)} > g_{(\gamma_n, \phi_n)} \tag{25}$$

where $R^n f$ is the n^{th} residue.

For the atom defined above, the Wigner-Ville distribution is:

$$WVD(t, \omega) = \frac{1}{2}(Wg(\frac{t-u}{s}, s(\omega - \xi)) + Wg(\frac{t-u}{s}, s(\omega + \xi))) \tag{26}$$

The time-frequency energy distribution of the reconstructed signal ends up being the sum of Gaussian chunks with locations and variances along the time and

frequency axes that are dependent on γ. The total signal energy is computed by adding the WVD distributions of selected atoms as shown in the equation below:

$$Ef(t,\omega) = \sum_{n=0}^{M} | < R^n f, g_{\gamma_n} > |^2 WVD_{\gamma_n}(t,\omega) \tag{27}$$

where M is the number of atoms used to approximate the signal (selected atoms).

As the analysis in this project is confined to signals to finite length (N), the decomposition is done on atoms of the same length too. Therefore, the atoms need to be periodized. The construction of a discrete atom of length N is done by summing g and its infinite copies that are shifted by a multiple of N and afterwards sampling the window function uniformly over N points to get a discrete and periodic signal at any scale s. This is given by the following equation:

$$g_s(n) = \frac{K_s}{\sqrt{s}} \sum_{p=-\infty}^{+\infty} g(\frac{n-pN}{s}) \tag{28}$$

where $\frac{K_s}{\sqrt{s}}$ is the normalization factor.

For any integer values $0 \leq p < N$ and $0 \leq k < N$, s values such that $s \in]1, N[$, and $\gamma = (s, p, \frac{2\pi k}{N})$, the discrete Gabor atom may be given as:

$$g_{\gamma_n} = g_s(n-p)e^{i(\frac{2\pi k}{N})n} \tag{29}$$

This provides a discrete complex Gabor dictionary.

However, the Winger-Ville distribution is symmetric for real atoms, therefore values need to be calculated only for frequency values 0 to N/2; the remaining values are mirrored images about N/2. This way the energy between 0 and N/2 adds up to unity. Also, in this case, the Hilbert space H is the set of infinite discrete signals that have a period N.

A.2.3 MP Flowchart

Below is a flowchart summarizing the key steps of a basic matching pursuit algorithm based on the descriptions provided in the sections above.

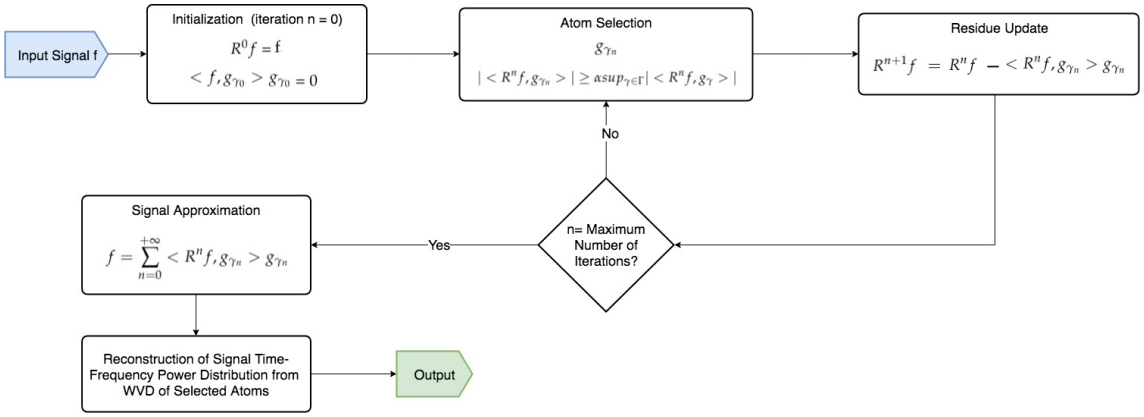

Figure 17: Basic Matching Pursuit Algorithm: an iterative algorithm attempts to approximate the signal f using functions (atoms) from an over-complete dictionary. A residue $R^n f$ represents the error after approximation. At the beginning $R^n f$ is set to equal the signal as the approximation at that point is equal to 0. In each iteration the best matching atom g_{γ_n} is selected to approximate part of the signal based on the inner product between the current residue and the atoms in the dictionary. Then the residue value is updated to produce the next residue value $R^{n+1} f = R^n f - approximation$, where the approximation is given by the product of the selected atom and its corresponding inner product. This is repeated until the maximum number of iterations is reached. The signal is decomposed into a linear expansion of atoms weighted by the inner product coefficients. Afterwards, the time-frequency power distributions for the selected atoms is reconstructed based on the Wigner-Ville distribution.